Technology Collaboration Programme
by iea

International Energy Agency
Photovoltaic Power Systems Programme

Task 17 PV & Transport

PVPS

PV System Technology Considerations for PV-Powered Passenger Vehicles

2026

Report IEA-PVPS T17-7:2026

What is IEA PVPS TCP?

The International Energy Agency (IEA), founded in 1974, is an autonomous body within the framework of the Organization for Economic Cooperation and Development (OECD). The Technology Collaboration Programme (TCP) was created with a belief that the future of energy security and sustainability starts with global collaboration. The programme is made up of 6.000 experts across government, academia, and industry dedicated to advancing common research and the application of specific energy technologies.

The IEA Photovoltaic Power Systems Programme (IEA PVPS) is one of the TCP's within the IEA and was established in 1993. The mission of the programme is to "enhance the international collaborative efforts which facilitate the role of photovoltaic solar energy as a cornerstone in the transition to sustainable energy systems." In order to achieve this, the Programme's participants have undertaken a variety of joint research projects in PV power systems applications. The overall programme is headed by an Executive Committee, comprised of one delegate from each country or organisation member, which designates distinct 'Tasks,' that may be research projects or activity areas.

The IEA PVPS participating countries are Australia, Austria, Belgium, Canada, China, Denmark, Finland, France, Germany, India, Israel, Italy, Japan, Korea, Lithuania, Malaysia, Morocco, the Netherlands, Norway, Portugal, South Africa, Spain, Sweden, Switzerland, Thailand, Turkey, the United Kingdom and the United States of America. The European Commission, Solar Power Europe and the Solar Energy Research Institute of Singapore are also members.

Visit us at: www.iea-pvps.org

What is IEA PVPS Task 17

The objective of Task 17 of the IEA Photovoltaic Power Systems Programme is to deploy PV in the transport, which will contribute to reducing CO2 emissions of the transport and enhancing PV market expansions. The results contribute to clarifying the potential of utilization of PV in transport and to proposal on how to proceed toward realising the concepts.

Task 17's scope includes PV-powered vehicles such as PLDVs (passenger light duty vehicles), LCVs (light commercial vehicles), HDVs (heavy duty vehicles) and other vehicles, as well as PV applications for electric systems and infrastructures, such as charging infrastructure with PV, battery and other power management systems.

SUGGESTED CITATION

Bittkau, K., Patel, N., Slooff-Hoek, L.H., Apaydin, R.O., Rosca, V., Mujovi, F., Faes, A., Chambion, B., Duigou, T., Araki, K. (2026). Bittkau, K (Ed.), *PV System Technology Considerations for PV-Powered Passenger Vehicles* (Report No. T17-07:2026). IEA PVPS Task 17. https://iea-pvps.org/key-topics/t17-technology-considerations-vipv-2026/

COVER PICTURE

Examples of VIPV - see Figure 2.1-2 for details.

INTERNATIONAL ENERGY AGENCY
PHOTOVOLTAIC POWER SYSTEMS PROGRAMME

PV System Technology Considerations for PV-Powered Passenger Vehicles

IEA PVPS
Task 17
PV and Transport

Report IEA-PVPS T17-7:2026
March 2026

ISBN: 978-1-923734-03-6
DOI: 10.69766/IYIK7476

AUTHORS

Main Authors

Karsten Bittkau, Forschungszentrum Jülich, Germany
Lenneke H. Slooff-Hoek, TNO, the Netherlands
Antonin Faes, CSEM, Switzerland
Bertrand Chambion, CEA, France
Kenji Araki, University of Miyazaki, Japan

Contributing Author

Neel Patel, Forschungszentrum Jülich, Germany
Ramazan Oguzhan Apaydin, TNO, the Netherlands
Victor Rosca, TNO, the Netherlands
Fahradin Mujovi, CSEM, Switzerland
Tatiana Duigou, CEA, France

Editor

Karsten Bittkau, Forschungszentrum Jülich, Germany

TABLE OF CONTENTS

List of abbreviations 8
Executive summary 10
1 Introduction 12
1.1 PV-powered passenger vehicles 12
1.2 Overview of PV system technology considerations 12
2 Curvature 13
2.1 A brief overview of curved PV manufacturing techniques 13
2.2 1D and 2D curvatures and its implications 15
2.3 Impact of curvature on PV performance and yield 18
2.4 Cell interconnection solutions for curved modules 20
2.5 Hotspots 21
3 Aesthetics 24
3.1 Aesthetics in terms of vehicle application 24
3.2 Overview of existing colouring techniques for different PV technologies 24
4 Weight 32
4.1 Influence of PV weight in PV-powered passenger vehicles 32
4.2 Case study 34
4.3 Results 36
5 Compliance and Safety 39
5.1 Overview of testing standards for PV and automotive sectors 39
5.2 Testing examples of different PV technologies 41
5.3 Special testing requirements for curved PV 42
5.4 Toxic materials 44
5.5 Vibration robustness 45
6 Conclusion 46
References 47

LIST OF ABBREVIATIONS

1D	One-dimensional
2D	Two-dimensional
ARC	Anti-reflection coating
BC	Back-contacted solar cells
BIPV	Building integrated photovoltaics
BoM	Bill of materials
CBF	Conductive back foil
CVD	Chemical vapor deposition
DC	Direct current
DCP	Digital ceramic printing
ECE	Economic commission for Europe
EV	Electric vehicle
EVA	Ethylene-vinyl acetate
FTB	Front-to-back contacted solar cells
GPS	Global positioning system
HDV	Heavy duty vehicles
IBC	Interdigitated back contact
IEA	International energy agency
IEC	International electrotechnical commission
ISO	International organization for standardization
LCV	Light commercial vehicles
MBB	Multi-busbar
MPP	Maximum power point
MQT	Module quality test
MST	Module safety test
OECD	Organization for economic cooperation and development
PERC	Passivated emitter and rear cell
PET	Polyethylene terephthalate
PLDV	Passenger light duty vehicles
POA	Plane-of-array
PT600	IEC project team for VIPV systems

PV	Photovoltaics
PVB	Polyvinyl butyral
RAL	Reichs-Ausschuss für Lieferbedingungen und Gütesicherung (Imperial committee for delivery and quality assurance)
RTE	Relative thermal endurance
RTI	Relative thermal index
TC	Thermal cycling
TCP	Technology collaboration programme
TI	Thermal index
SEPA	Smart electric power alliance
SHJ	Silicon heterojunction technology
STC	Standard test conditions
UV	Ultraviolet
V2X	Vehicle-to-X
VAPV	Vehicle applied photovoltaics
VIPV	Vehicle integrated photovoltaics

EXECUTIVE SUMMARY

This report provides a comprehensive overview of Vehicle Integrated Photovoltaic (VIPV) systems, focusing on their technological considerations, challenges, and potential applications in the automotive industry. The report covers various aspects of VIPV, including curvature, aesthetics, weight impact, compliance, and safety.

- **Curvature**: The integration of photovoltaic (PV) modules onto curved vehicle surfaces presents unique challenges. Researchers have explored various manufacturing techniques for both Vehicle Applied PV (VAPV) and Vehicle Integrated PV (VIPV). The report discusses the mechanical behavior of PV cells under double curvature, providing insights into the limits of cell bending to avoid cracks and electrical losses. The impact of curvature on PV performance and yield is also examined, highlighting the need for optimized electrical topologies in curved modules.
- **Aesthetics**: The report emphasizes the importance of aesthetics in VIPV applications, particularly color and surface finish. Various coloring techniques for different PV technologies are presented, including coloring of rear-side materials, solar cells, front encapsulants, and front materials. The report also discusses the challenges of color reproducibility and the demand for specific RAL colors in VIPV applications.
- **Weight Impact**: The additional weight of onboard PV systems is a critical factor in evaluating the energy benefits of PV-powered vehicles. The report presents a methodology to assess the impact of PV weight on the energy balance of electric vehicles, introducing the concept of a yield factor. Case studies involving different PV technologies and vehicle models demonstrate that the impact of PV weight is significant but can be offset by energy yield during parking phases.
- **Compliance and Safety**: The report outlines the current lack of dedicated standards for VIPV and addresses a safety qualification program based on existing PV and automotive standards. This program combines elements from IEC 61730-2:2016 and ISO 16750, along with additional tests specific to VIPV applications. The report also discusses recent updates to relevant standards and their implications for VIPV testing.
- **Testing Considerations**: Special testing requirements for curved PV modules are highlighted, emphasizing the need for reproducible testing methods. The report presents findings from international round-robin projects involving testing laboratories and research institutes, revealing challenges in measuring curved modules and the importance of considering indoor test results versus outdoor performance for VIPV products.
- **Toxic Materials and Vibration Robustness**: The report briefly mentions the potential use of toxic materials in VIPV systems and the importance of considering political regulations and recyclability. Vibration robustness is identified as a significant risk for long-term reliability, with the report discussing the limitations of current damping materials in the frequency ranges relevant to vehicle applications.

Key Takeaways:

- VIPV technology presents unique challenges in terms of curvature, aesthetics, and weight impact that require careful consideration during design and implementation.
- Standardization efforts are ongoing to develop comprehensive testing and safety qualification programs specific to VIPV applications.
- The energy balance of PV-powered vehicles depends on various factors, including PV technology, vehicle type, and usage patterns.
- Aesthetic considerations, particularly color and surface finish, play a crucial role in the acceptance and integration of VIPV systems.
- Special testing methods and considerations are necessary for curved PV modules to ensure accurate performance evaluation and long-term reliability.

Future Outlook:

As VIPV technology continues to evolve, further research and development are needed to address the challenges identified in this report. Standardization efforts, improved testing methodologies, and advancements in PV technologies tailored for vehicle integration will be crucial in realizing the full potential of VIPV systems in the automotive industry. In particular, road authorities have their own quality tests for safety requirements. VIPV performance and energy yield evaluation require much more input data, including the commute pattern, without having any standard that allows a comparison between different VIPV systems.

1 INTRODUCTION

1.1 PV-powered passenger vehicles

To counteract man-made climate change, strong effort has to be made in all application sectors. This also requires the electrification of the transport sector leading to significantly higher electricity demand. Integrating photovoltaic (PV) systems into existing structures (buildings, roads, vehicles, agricultural areas, etc.) helps to reduce the total areas needed for generating the electricity to meet the increasing demand. In the transport sector, the PV system might be added on top of the vehicle (VAPV – vehicle applied photovoltaics) or fully included into the vehicle body (VIPV – vehicle integrated photovoltaics). The electricity generated by the PV system might be used to directly power the vehicle during its driving, charge the battery during parking state, or fed to the grid or other devices (V2X – Vehicle-to-X).

Among other PV applications, PV-powered passenger vehicles require special technology considerations due to their unique nature. Those considerations are introduced in the next section.

1.2 Overview of PV system technology considerations

The technology considerations, as studied in this report, are categorized by different aspects, as illustrated in Figure 1.2-1. The curvature of the vehicle's body is considered in Chapter 2 in terms of mechanical stability of the PV modules and the impact of the curved shape on their performance. Visual appearance of VIPV modules plays a key role in the social acceptance. Different colouring technologies for PV are discussed in Chapter 3 with respect to their applicability, homogeneity, and impact on the PV performance. With the VIPV system, the vehicle has to move additional weight due to the modules and the electronics, which increases the energy consumption. The overall energy balance for different VIPV solutions is investigated in Chapter 4. Finally, compliance and safety issues of VIPV systems is summarized in Chapter 5.

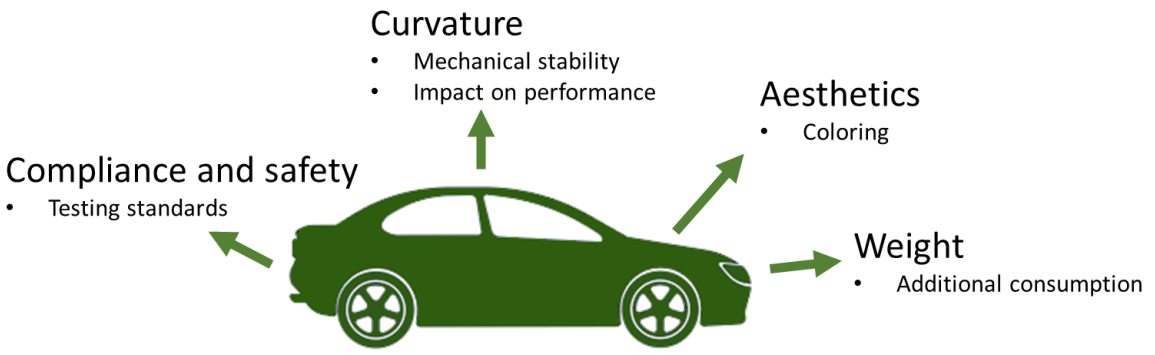

Figure 1.2-1 Concept figure showing the technology considerations investigated in this document.

2 CURVATURE

2.1 A brief overview of curved PV manufacturing techniques

Photovoltaic (PV) module manufacturing is crucial to safeguard the long lifetime of solar cells and therefore solar power production. Because these panels are exposed to different environmental conditions, the choice of materials (bill of materials- BoM) and methodology for manufacturing gain ample importance [1] [2]. In addition, when applied on vehicles, non-standard shapes (curvature of the parts), additional mechanical forces (i.e. vibrations) impacting on the car body, and therefore on the solar panels, bring more complexity in the material choice, design (both geometry and electrical), assembly, processing and installation of PV modules [1] [2] [3] [4] [5] [6]. Consequently, the use and installation of solar cells or PV modules on these complex car parts can often be a major challenge. In this regard, researchers have explored various routes towards realizing installation of PV components on vehicles. In this report, we summarise this topic under two main sections.

2.1.1 Integration onto the vehicle - Vehicle applied PV (VAPV)

Vehicle applied PV elements are components that are attached to the car body in various manners. These panels are usually produced using lightweight flexible materials; however, conventional PV panel applications are also present. There are two simple solutions in order to apply PV on the vehicle body. These are (a) using screws, brackets or rails to fix the PV component and (b) adhesive method (gluing, sticking using for example double-sided tapes onto the car body or magnetic attachment) [7] [8]. The former, which is more flexible and adjustable, is generally used for conventional PV panels whereas it increases the weight of the car. The latter is used for flexible panels that can follow the shape of the vehicle part. This however results in increased height and wind resistance as well as module related problems (i.e. cell cracks) depending on the geometry. Figure 2.1-1 shows some examples of VAPV on different vehicles.

a)  b) 

Figure 2.1-1 VAPV examples on various vehicles (a) PV panel installed on racks [7], (b) PV panel attachment on roof with magnetic rear panel [8]

2.1.2 Integration directly into the car body – Vehicle integrated PV (VIPV)

The term VIPV refers to the installation of a PV module directly into the roof or hood and sometimes on the trunk or doors of a vehicle. In this approach, the corresponding part of the vehicle body is used as a fixed part of the PV module. For example, in the case of glass roof applications, the glass roof of the vehicle can be used as the protective front glass that is used in conventional modules. Similarly, a metal body part of a vehicle can be used as a rigid

substrate providing the mechanical durability and stability to the module. Such PV integrated vehicle components can be realized in different ways.

Standard lamination procedures that are used for conventional modules can be adopted for manufacturing curved PV components whereas, alternatively, autoclave or oven lamination approaches are also considered [1] [9]. In these approaches, pre-shaped rigid and/or flexible counterpart combinations (rigid-rigid or rigid-flexible) are used to support and protect solar cells. The cells can be placed on the supporting/protecting body part as single cell, cut-cells, strings of cells, shingled cells, thin film cells or combinations depending on the geometry, design and expected power output. In Figure 2.1-2, some examples of such applications are shown.

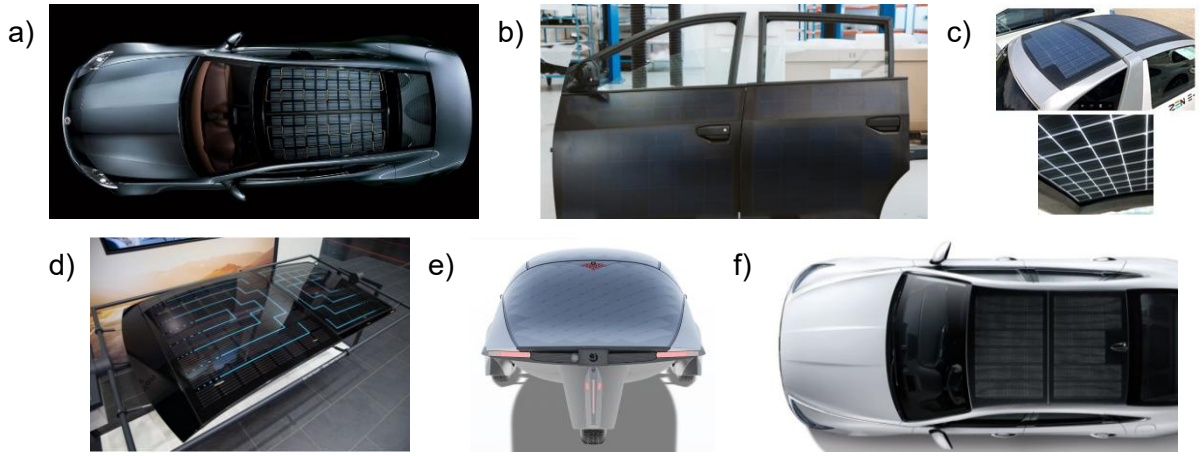

Figure 2.1-2 Examples of VIPV elements (a) PV car roof from a2-solar on the Fisker Karma [82], (b) car parts with integrated solar cells from Sono Motors [83], (c) integrated PV panels on Courb C-Zen body [84], (d) solar panel system for car roofs [85], (e) Aptera Solar Electric Vehicle [86], (f) Hyundai solar car roof [87]

In addition, VIPV applications can be based on an integrated approach as described in [10] [11] [12]. In this approach, smaller glass-free and robust semi-fabricates (intermediate products), similar to thin film PV sheets or building integrated photovoltaics (BIPVs) foil products [13] [14] [15] are produced. These semi-fabricates are designed to have defined electrical characteristics enabling a configurable system output via series or parallel connections with the neighboring semi-fabricate, and to be readily integrated into the final PV product in a secondary process step. Figure 2.1-3 shows a representation of the semi-fabricate processing into a final product [12].

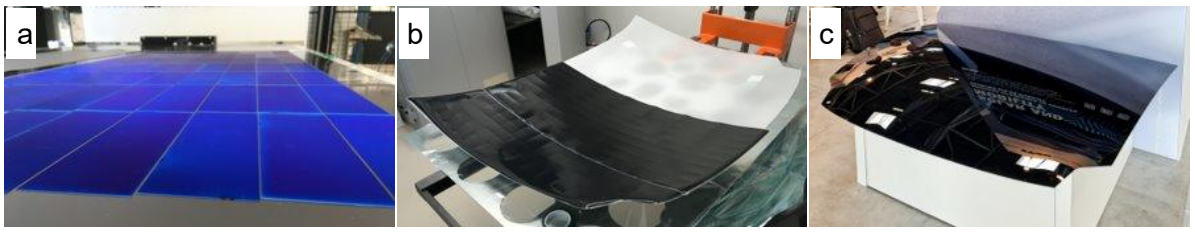

Figure 2.1-3 Semi-fabricate processing (a) and integration (b) and final product (c - car hood)

Flat modules with flexible components can also be applied on curved surfaces. There are several companies that are producing flexible PV panels that can be applied on surfaces with 1D (cylindrical shape).

In the majority of cases, flexible panels designed for use on 1D curve surfaces demonstrate a lack of conformity when employed on 2D curve surfaces. To apply flat PV on 2D curved surface, dedicated cut lines within a flat & thin PV module could be used [16] [17]. It results in a conformable PV module, that can be installed on different types of roofs. The module is built flat on a polymer base (front side PET and back side nitrile rubber with magnetic ferrites). The mechanical design of the module allows for partial cutting of the module between the PV cell strings and thus greatly increases the conformability of the module on different curved surfaces. This kind of PV module is well adapted for electric vehicle solarisation kits or lightweight vehicles. In Figure 2.1-4, a design of a conformable PV module with partial cut is shown. Figure 2.1-5, show the resulting panel after installation onto Renault Zoe roof.

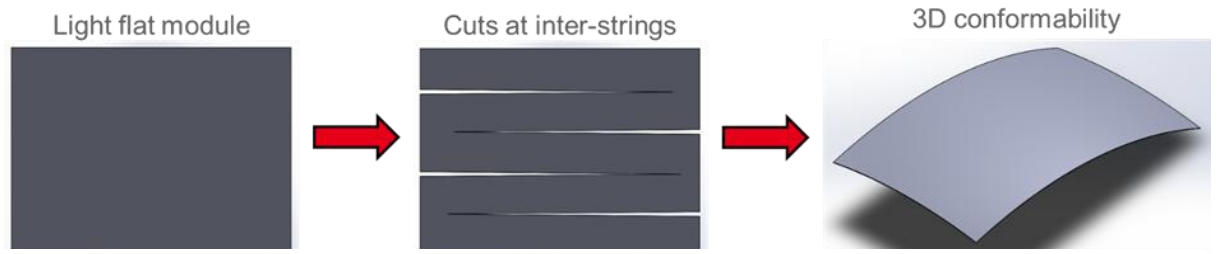

Figure 2.1-4 Conformable PV module design from light flat module to 3D conformability.

Figure 2.1-5 Global view of a Renault Zoe vehicle with 145 Wp module on roof top.

2.2 1D and 2D curvatures and its implications

In order to consider curved PV panels on vehicles, the first step is to focus on the mechanical behaviour of photovoltaic cells when bent under double curvature (2D). This will enable to define curvature radii for the integration of PV cells into double curved PV modules. The finality is to define limits, to avoid cells cracks, and the electrical losses they imply. Duigou et al proposed a combined methodology, including numerical and experimental approaches [18]. The experimental part of the study focussed on mechanical failure of full and half M2 cells

under spherical curvature. A set of experimental tests was performed to obtain a "pass-or-fail" criterium on the allowed shapes (i.e. minimum spherical radius). The limiting shape will enable to get a value of the maximum tensile stress allowed for a cell without interconnection ribbons. The implementation of a numerical model allows for the analysis of principle stresses in the cell under spherical curvature and double curvature. The influence of several parameters must be considered, such as cell's area, thickness, and shape factor on the limit allowed shape. The term "shape factor" will refer to the ratio of width over length of the cell. For example, a third of cell has a shape factor of 1/3 and a half-cell, a shape factor of 1/2.

The numerical model aims to curve silicon cells in spherical shape. Material data that are considered for silicon are presented in Table 2.2-1. The ultimate tensile stress of the considered cells can be estimated to be around 120 MPa [19]. This value will be used as an input in the numerical study.

Table 2.2-1 Material data for Silicon as input for mechanical modelling [19]

Measurement	Unit	PV cell
Density	kg/m^3	2330
Poisson ratio	–	0.28
Young modulus	GPa	See eq. 1
Tensile ultimate stress	MPa	120

$$\begin{bmatrix}\sigma_{xx}\\ \sigma_{yy}\\ \sigma_{zz}\\ \tau_{xy}\\ \tau_{yz}\\ \tau_{zx}\end{bmatrix} = \begin{bmatrix}166 & 64 & 64 & 0 & 0 & 0\\ 64 & 166 & 64 & 0 & 0 & 0\\ 64 & 64 & 166 & 0 & 0 & 0\\ 0 & 0 & 0 & 80 & 0 & 0\\ 0 & 0 & 0 & 0 & 80 & 0\\ 0 & 0 & 0 & 0 & 0 & 80\end{bmatrix} \begin{bmatrix}\epsilon_{xx}\\ \epsilon_{yy}\\ \epsilon_{zz}\\ \gamma_{xy}\\ \gamma_{yz}\\ \gamma_{zx}\end{bmatrix} \quad (1)$$

The existence of tensile stresses at the centre of the cell should also be underlined: shaping a non-developable surface on a sphere implies the apparition of compressive stresses at the periphery, while central areas undergo tensile effects, especially in the direction ±45°. By testing several thicknesses and radius of curvature in the numerical model, a reference curve with two zones was obtained: a breakage area and a safe zone (Figure 2.2-1).

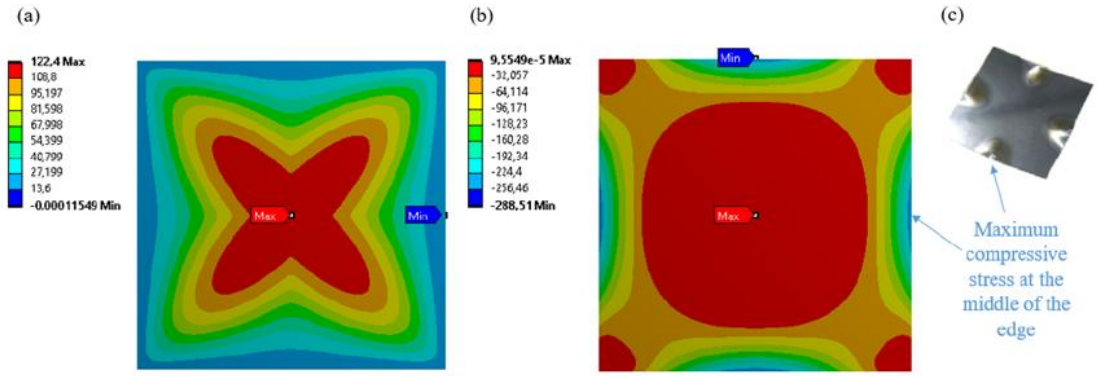

Figure 2.2-1 Map of the stresses for a complete cell under spherical curvature (R = 800 mm, thickness = 180 µm), in MPa. (a) Maximum principal stresses S1. (b) Minimum principal stresses S3. (c) A picture of a wafer undergoing buckling at the middle of its edges under double curvature load [88]. This area numerically corresponds to an area of maximum compressive stress.

To complement the numerical study, a set of experimental tests was led on non-interconnected cells, to validate the allowed double curved shapes estimated with the numerical model. For each case the cell is pushed in contact to a curved mold thanks to hydrostatic pressure to conclude on a failure or passed test. These results are integrated in Figure 2.2-2.

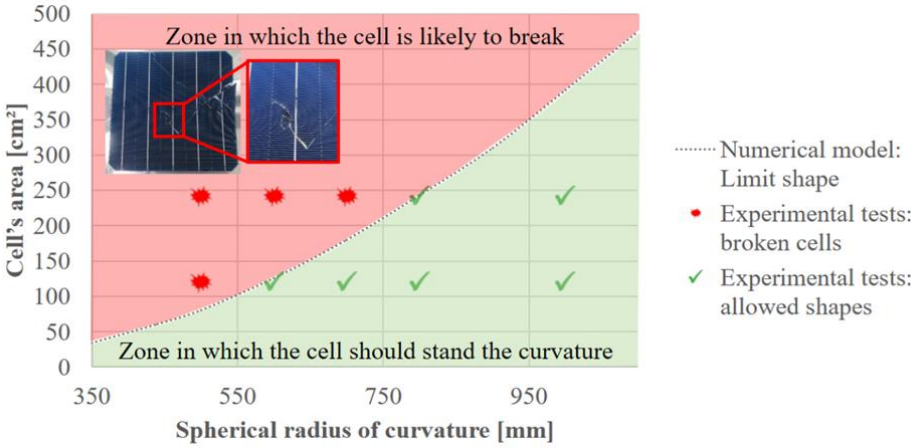

Figure 2.2-2 Relation between the spherical radius and the maximum allowed area: "allowed" and "forbidden" zones for a square cell with thickness 180 µm. The dot line corresponds to the limit shapes, for which $S1_{max}$ = 120 MPa. Results of the experimental tests points are represented, as well as an example of a broken cell. The break occurs near the centre of the cell.

The methodology was deployed on larger cells (up to M12), half and third formats. It gives new mechanical limits for cell bending (Figure 2.2-3). Compared to full cells, half cut cells have the same limits, but third cut cells give a significant advantage for bending.

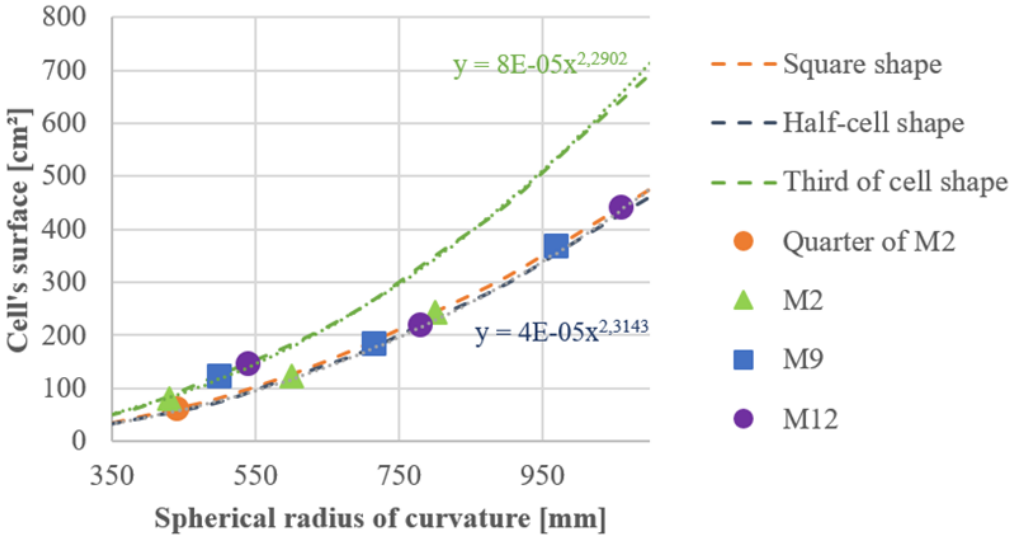

Figure 2.2-3 Break limit depending on the geometry and area of the cell.

This study explores the theoretical limits of PV cell mechanical integrity under spherical bending, providing a foundation for the design of optimal cell packaging configurations within the context of VIPV applications. However, it is imperative to note that these considerations must be adapted in accordance with the specifications of the packaging, the interconnects employed, and the manufacturing process.

2.3 Impact of curvature on PV performance and yield

Curved PV modules are already used on the market in VIPV implementations (Toyota Prius as example [20]) but characterization procedure and tools are still lacking. Providing such tools might in fact prove to be challenging as curved modules bring many layers of complexity. To solve this issue, the work group PT600 is currently undertaking the task to properly set a norm for VIPV modules. An appropriate norm would allow to establish a common ground between different curved modules performance wise and price wise.

Proportionally to the curvature level of the module, the irradiance should be inherently inhomogeneous over the module's cells. By having a different level of irradiance, each cell's current, and thus power, output will vary. In a complex module design, using bypass diodes and complex topologies, it becomes clear that the curvature will impact the module performances and yield.

From the least to the most curved setting depicted in Figure 2.3-1, the I_{SC} measured are 5.9 A, 5.9 A, 5.6 A and 5.17 A. Looking at the Table 2.3-1, the irradiance difference corresponds to a very similar difference in I_{SC}.

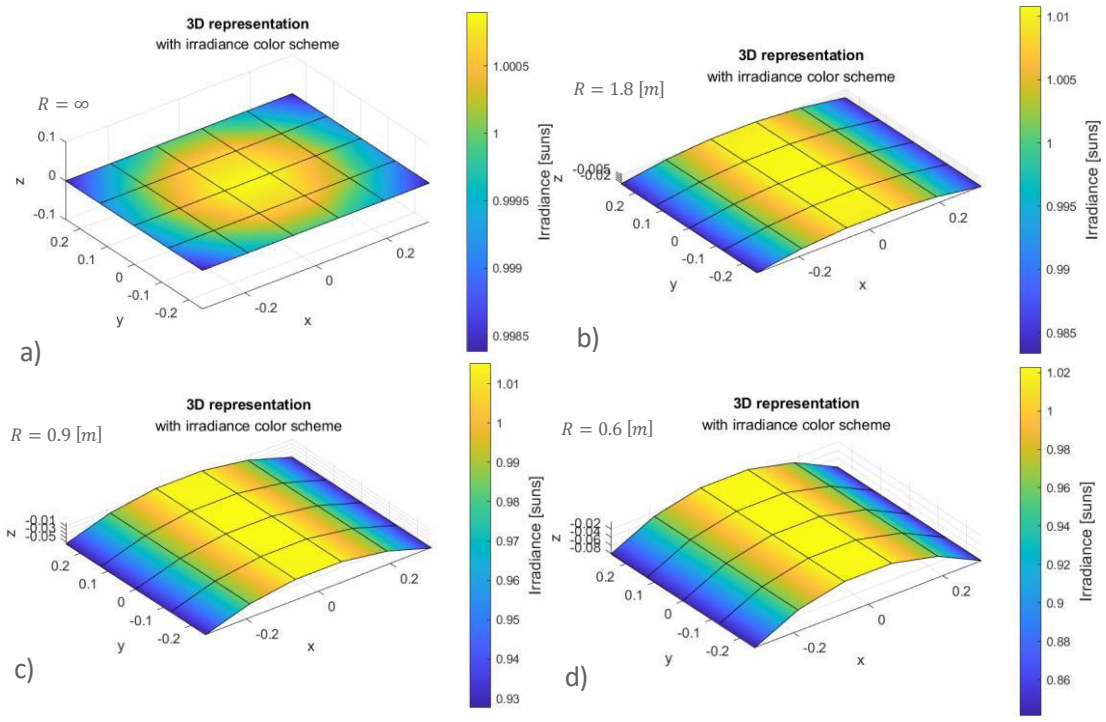

Figure 2.3-1: Simulated irradiance with the PASAN 8 m light source for different curvature levels. Each point on the graph represents a solar cell, totalling 60 cells.

Table 2.3-1: Comparison of the normalized (compared to the flat reference) I_{SC} and irradiance for each curvature level. The two values are indeed correlated and illustrate how the current is limited by the lowest irradiated cells in the module. The slightly higher values of current compared to the irradiance come from the fact that the other cells which are more irradiated still influence the overall I-V curve. When the curvature increases, the difference in irradiance follows the same trend.

Radius [m]	$I_{SC}/I_{SC,ref}$	$Irrad/Irrad_{ref}$
∞	100%	100%
1.8	98.8%	98.7%
0.9	94.5%	93.4%
0.6	85.8%	84.6%

As we see, curvature can greatly impact the maximum power output of a module. One potential improvement can come from optimizing the electrical topology of a curved module which might be useful to properly use the power of each string as their current might often be mismatched. This condition heavily depends on the module itself and the environment in which it will be used, and having a tool capable of predicting the result would result in a facilitated optimization during its design phase. Some examples are shown below.

As shown on Figure 2.3-2, the measured I-V curve is impacted by the curvature level mainly on the short-circuit current I_{SC} and by extension the P_{MPP}. Without bypass diodes, the limiting factor in a module connected in series is the cell that has the lowest irradiance. The low irradiance cell will impose the corresponding current to the complete module. In Figure 2.3-1, each curvature level will induce a proportional reduction in I_{SC} and P_{MPP}. As expected, the V_{OC} does not change very much: a change in irradiance only contributes in a logarithmic way to the V_{OC}. Moreover, the highest change in voltage happens across the edge strings (with the lowest irradiance) only, not across the complete module as it is the case with the current, further minimizing the impact.

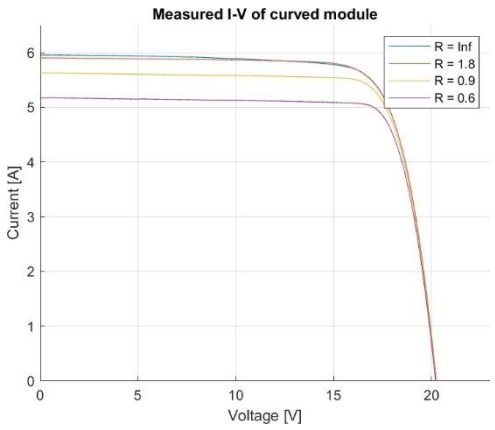

Figure 2.3-2 I-V curves of the module from Figure 2.3-1 flashed in a PASAN 8 m tunnel flasher without bypass diodes at different radii of curvature. The I_{SC} of the module is proportional to the I_{SC} of the string with the lowest irradiance, as it will be the limiting element of the overall performances

The measured I-V curves in Figure 2.3-2 correspond to different curvature levels as shown in Figure 2.3-1. As explained previously, the less irradiance the current limiting cells receives, the smaller the I_{SC} will become. This is perfectly illustrated in the following figure.

A common way to compensate for the mismatch in current between different strings is to use bypass diodes. By bypassing strings, the diode will allow the difference between each string to be compensated. As shown in Figure 2.3-3, this is reflected on the I-V curve by having a "step-like" effect. The strings subject to the lower irradiance levels will not limit other strings anymore as their bypass diode will effectively offer another path for the higher currents to flow through.

Even under clear sky conditions, the bypass diodes embedded in a module might continuously work and conduct current due to this effect. It becomes important to account for this when designing and selecting the diodes to be used in a curved module as their lifetime might be overestimated if compared to the normal behaviour you would see in a flat panel.

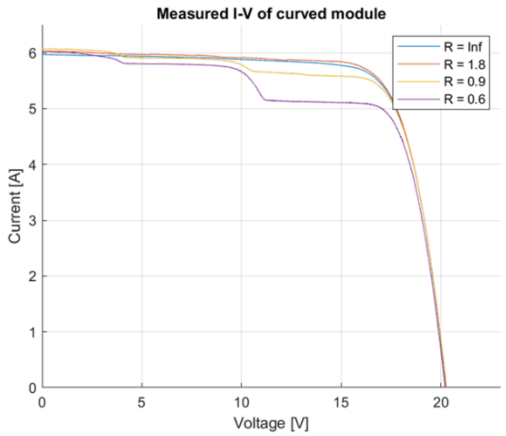

Figure 2.3-3: I-V curves of the same module as in Figure 2.3-2 but with each of its string bypassed with a diode. The module having six strings and the irradiance being symmetrical at the centre of the module, three levels of current are identified for each curve.

2.4 Cell interconnection solutions for curved modules

Regarding the choice of the cell type (back contact or front-to-back cSi) and the interconnection technology for manufacturing of the curved PV laminates, the following have to be considered: the maximum achievable power density (PV active area); electrical design flexibility (cell size, cell lay-out); aesthetics; and the stability of the interconnect under thermo-mechanical stresses during the manufacturing process and relevant simulated and real-life conditions. As for the interconnection technologies, we shall consider the tabbing and stringing of the multi-busbar (MBB) front-to-back (FTB) or back-contact (BC) cells; interconnection of the BC cells using a conductive back foil (CBF); and shingling.

The utilisation of tabbing for the purpose of connecting MBB FTB cells suggests the employment of a diversified supply chain, which may result in the most economical material cost. The adoption of unidirectional cells, reducing them to quarter cells, enables a certain degree of flexibility in defining the module's output, as well as the cell string length and

topology. However, the cell spacing required by the interconnection method (typically between 2 and 3mm), the linear topology of the string, and the additional space required for the bussing, make it rather challenging to approach the cell packing density of a standard module. Furthermore, it is essential to ensure a good fit between the size of the (cut) wafer and the available surface area to achieve a reasonably high cell packing density. Finally, and perhaps most importantly, cells connected in strings by means of soldering will experience additional thermo-mechanical stresses during the assembly and final lamination steps. It is also noteworthy to mention the ribbon tiling technology, which has the capacity to eliminate the intercell spacing in a string and thus maximise the power density [21].

Cell shingling represents an interconnection method that achieves higher cell packing densities and eliminates thermo-mechanical stresses associated with the utilization of soldered ribbons. However, it is important to note that achieving higher cell packing densities does not necessarily imply higher power density, as this is contingent on the efficiency losses associated with cell cutting. The manufacturing of curved VIPV shingled laminates is still problematic due to the occurrence of mechanical stresses and cell breakage during cell cutting, module assembly and lamination. However, there are reports [22] [23] of good resilience in thermal cycling and a low cell breakage rate for standard flat shingled modules. It is crucial to note that cells intended for utilisation in shingled modules necessitate dedicated metallization processes that are optimised for shingling. Finally, it may be argued that shingled modules offer an aesthetically superior solution by virtue of the elimination of ribbons.

The CBF-based BC module employs a conductive layer and a suitable interconnect (Electric Conductive Adhesive or Low Temperature Soldering) to connect BC cells in groups [24]. The inherent benefits of this interconnection technology include the ability to achieve higher cell packing density (intercell distance reduced to 0.5 mm [25] and customized module shapes [26]. Furthermore, this method allows for an easy interconnection of the (cut) cells of virtually any size and shape, thereby enhancing the potential for achieving advanced electrical module topologies that improve yield, shade tolerance, and VIPV system safety [27]. Concerns have been raised regarding the robustness of the supply chain for BC cells and CBF, and the potential consequences of higher material costs.

In conclusion, it is asserted that the most significant design consideration when selecting interconnection technology is the capacity to realise optimum electrical topologies for VIPV. These topologies require the possibility to split the module into a large number of smaller cell groups/strings [28].

2.5 Hotspots

Due to the unconventional configurations that VIPV modules may adopt, the conventional assumptions made in standard analyses must be re-evaluated in the context of hotspots. The advent of novel cell technologies, characterised by exceedingly low breakdown voltages (reaching as low as a few volts per cell), has the potential to profoundly alter the role of bypass diodes in the context of hotspot prevention.

In the case of a shaded (or non-functional) cell, the current is typically impeded from passing through it, thereby preventing the entire string of cells from generating current. However, in more extreme cases, the shadowed cell can be reverse biased to such a degree in negative voltages that it reaches its reverse breakdown voltage and current is permitted to pass through it. In such instances, the cell does not generate power; rather, it dissipates energy in the form of heat.

The deployment of bypass diodes is instrumental in averting such a scenario by enabling the current to circumvent the shadowed cell. It is important to note that even with the implementation of bypass diodes, shadowed solar cells may still exhibit reverse breakdown behaviour [29].

Usual c-Si cells can have breakdown voltages V_{BD} between -15 to -20 [V]. In standard module, one usually finds that the number of cells one diode can bypass is at most around 26 cells. More than that, and it is expected to have a hotspot in case of a single cell shadowing. From Kirchhoff equations, if we take a string consisting of n solar cells, bypassed by a single diode, we can extract the condition illustrating the maximum number of bypassed cells n_{max}, right before the reversed biased shadowed cell reaches its breakdown voltage. With the following parameters:

$$V_{\mathrm{BD}} \cong 18\ [\mathrm{V}]^{1}$$

$$V_{\mathrm{OC}} \cong 0.68\ [\mathrm{V}]$$

$$V_{\mathrm{Fdiode}} \cong 0{,}4\ [\mathrm{V}]$$

We can extract n_{max} and obtain:

$$n_{\mathrm{max}} < \frac{V_{\mathrm{BD}} - V_{\mathrm{F}}}{V_{\mathrm{OC}}} + 1$$

$$n_{\mathrm{max}} < 26$$

This is the standard case and by bypassing less than ~26 cells (even less to account for a safety margin), the risk of hotspot can be mitigated. Now, computing this same result but by considering the breakdown voltage of an IBC cell that would be $V_{BD} = 5\ [V]$, we obtain a maximum number of cells to bypass:

$$n_{\mathrm{max}} < 7$$

Using cells with a lower breakdown voltage indicates that the maximum number of cells to bypass with a diode will also be lower. The relationship being nearly linear, with

$$n_{\mathrm{max}} \propto \frac{V_{\mathrm{BD}}}{V_{\mathrm{OC}}}^{2}$$

This showcases how different cell technologies, placed in the same configurations (topology, bypass diodes number and placement, etc…) can hugely impact the risk of hotspots.

Finally, hotspot occurring on cell with different breakdown voltages will heat up to different temperatures. By estimating the dissipated power in a cell in reverse breakdown voltage with:

$$P_{\mathrm{dissipated}} \cong I_{\mathrm{cell}} \cdot V_{\mathrm{BD}}$$

It has been demonstrated that the power is directly proportional to the breakdown voltage. Consequently, a cell with a lower breakdown voltage is expected to generate less heat, in

[1] The breakdown voltage is always negative, here, depending on how the voltage is represented on the electrical schematic, it can be shown positive. If it is given negative, a minus sign needs to be added in front of the V_{BD} in the equation.

[2] This relation becomes less valid the lower V_{BD} becomes.

accordance with this relationship. This finding also suggests that cells producing less current would likely dissipate less power. However, this assertion is frequently countered by the observation that the available surface area for heat dissipation through thermal conduction is often diminished (in the case of cut cells). Figure 2.5-1 illustrates two panels, manufactured for the same goal with very different cell technologies. As their breakdown voltages differ by more than 20 V, the temperature at which each heats up in hotspot conditions will also differ greatly.

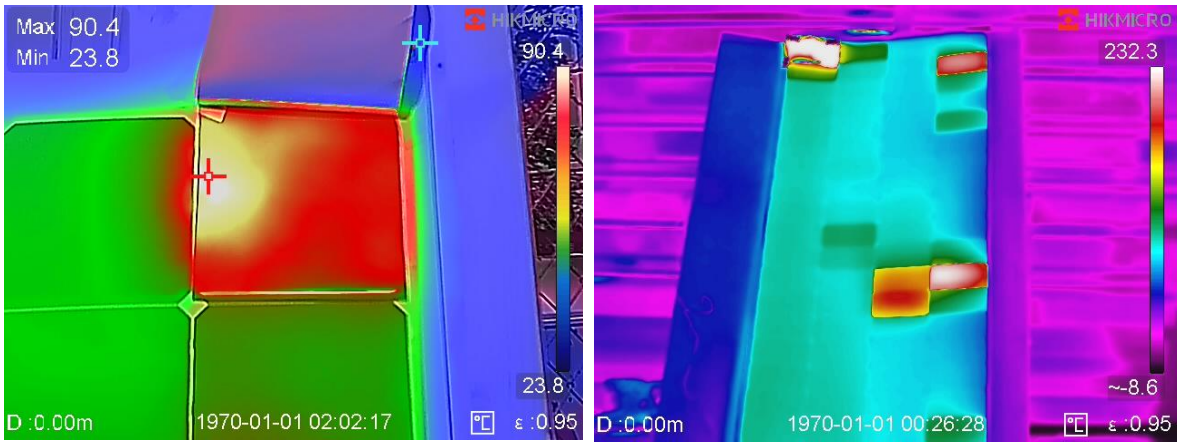

Figure 2.5-1: Two panels with similar designs made using different cell technologies. Left: panel made with very low breakdown voltage SunPower cells of $V_{BD} \cong 5$ V. The observed maximum temperature was of $90°C$. Right: panel made with high $V_{BD} \cong 20$ V PERC cells. The observed temperature was much higher at $\sim 230°C$.

The Sunpower panel exhibited a hotspot temperature that did not compromise the panel's or encapsulant's integrity, while the PERC panel's hotspot inflicted significant damage.

It is important to note that the behaviour of the hotspot can also be influenced by the environmental temperature, the temperature of the adjacent cells, and the thermal conductivity of the panel (i.e. the efficiency with which the panel dissipates the heat generated by the hotspot). Furthermore, the complexity of hotspots increases with partial cell shading, which complicates their prediction.

3 AESTHETICS

3.1 Aesthetics in terms of vehicle application

Task 17 of the IEA-PVPS has reported on a survey among experts to get insight in the important aesthetic aspects of [30]. The survey results indicate that approximately 25% of respondents consider color to be of significant importance in the application of PV in vehicles, while an additional 25% regard it as important. Furthermore, approximately half of the respondents expressed a desire for additional color options beyond the conventional deep blue and black hues typically employed by standard panels. On the other hand, half of the respondents expressed that efficiency is very important, with an additional 40% considering it to be important. This underlines the importance of highly efficient VIPV products that incorporate color. In addition to color, the visibility of the solar cells is also an important factor in aesthetic considerations. The ranking of the different cell connection options demonstrates that cell technologies with invisible interconnections, such as interdigitated back contact and Metal Wrap Through, are highly regarded, followed by multiwire and shingling, which exhibit more visible connections. Cells with visible busbars are found at the bottom of the ranking. The surface finish of the cells is also found to have a significant impact on their overall aesthetics. In the survey, respondents were invited to select a surface finish for various surfaces relevant to VIPV: roof, doors, bonnet, trunk. The options available were a matt or glossy finish. The roof surface exhibited a balanced preference for both finishes, while the remaining surfaces demonstrated a pronounced predilection for the matte option. This preference is likely influenced by the prevailing trend towards matt finishes in the automotive industry.

3.2 Overview of existing colouring techniques for different PV technologies

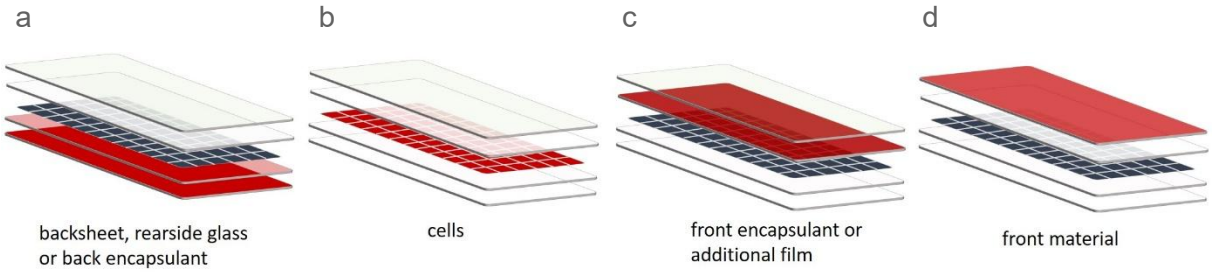

Figure 3.2-1 Possible positions of coloured layers in PV module stack. The red layers indicate the position in the module stack.

The availability of coloured PV has increased enormously in recent decades, driven by the need to have aesthetically pleasing PV panels for specific applications, such as facades and tilted roofs. The colouring technology utilised by different producers varies. Initially, the colouring was obtained by modifying the properties of the anti-reflection coating on the solar cells, thereby inducing metal-like colours. Since these pioneering days, a multitude of approaches to colouring PV panels has emerged. These methods differ in the position of the coloured layer in the module layer stack, as well as the manner in which the colour is applied

to that layer. Figure 3.2-1 provides an overview of the layers in a PV module and the locations for applying colours. Some examples are shown in Figure 3.2-2.

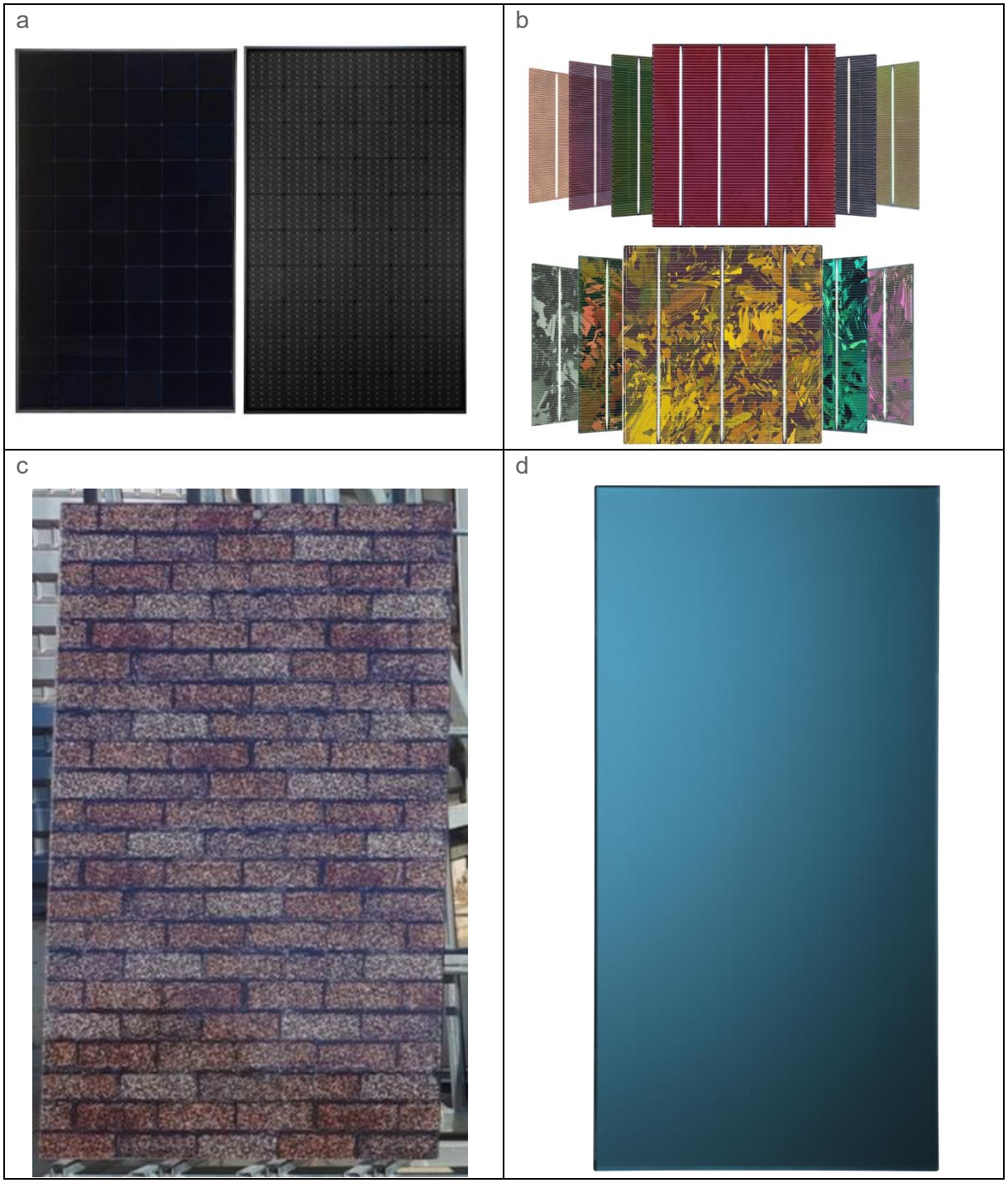

Figure 3.2-2: Examples of visual appearance of different ways of applying colour to PV modules. a) Energyra® IconIQ Full black with IBC cells and EclectIQ with PERC cells, b) coloured cells classic and marble series LOF Solar Corp, c) Solar Visuals, d) Kromatix Blue GT-215

The paragraphs below describe the following aspects of these colouring options:

- *Colour homogeneity* is very important when a manufacturer aims for a homogenously coloured module. In that case both the homogeneity within the module as well as the reproducibility of the colour between modules needs to be well controlled. An important issue for VIPV is the exact matching of the colour to existing colours in automotive. If the colour is slightly different from the other car body parts, it will in general not be accepted.
- *Angular colour stability*
- *Module performance* reduction due to the application of colours

3.2.1 Colouring of rear side material or rear side encapsulant

When looking from the bottom upwards, the first option for applying colour is the back sheet or rear glass, see **Error! Reference source not found.**a. This option has the benefit that it does not affect the efficiency of the module, as it is behind the solar cells.

The second option is to colour the encapsulant between the back sheet/rear glass, and the cell.

These options will only give a homogeneous appearance of the module if the back sheet, rear side glass or the encapsulant matches the colour of the solar cell, which in general will be dark blue or black. It will thus not be possible to generate homogenously looking PV modules in other colours unless the cells are also coloured. As there are often slight colour differences between different cells, this option will not give a very homogeneous colour within the modules as well as between different modules.

This colouring technique is showing good angular colour stability.

3.2.2 Colouring of the solar cells

The application of colour to the cells is achieved through the modulation of the thickness of the anti-reflection coating (ARC) on the cell. In that case the coating is not optimised for minimizing the reflection, but for obtaining a specific colour. The application of these coatings can be achieved through various methods, with the most prevalent being the chemical vapour deposition process (CVD). The colour reproducibility is predominantly influenced by the thickness variability of the ARC layers. In homogeneous cells, such as mono c-Si or a-Si cells, the ARC colouring produces relatively homogeneous colours, but in multi c-Si cells, the crystal structure of the cells remains visible. It is also crucial to select a back sheet (or "back encapsulant") that matches the colour of the cells in order to ensure a uniform colouration across the entire module.

This technique relies on the interference between different light beams that reflect from the various interfaces in the anti-reflection coating, resulting in a colour depending on the angle at which the observer views the panel.

3.2.3 Colouring of front encapsulant or additional film

The colouration of the front encapsulant is a relatively straightforward method of applying colour. A range of colours is offered by several encapsulant manufacturers. However, it should be noted that this method of colour application can result in a reduction in module efficiency relative to a non-coloured module, owing to the enhanced absorption characteristics within the encapsulant.

The manufacturing process of coloured encapsulants involves the use of extrusion, employing a base resin and a masterbatch. The masterbatch comprises concentrated pigments and additives enclosed in a carrier resin. The creation of this masterbatch entails the precise measurement of pigments and additives, their pre-mixing with a carrier resin, and their processing in either a twin-screw extruder or a compounder. The extruded resin, containing the pigments and additives, is then subjected to cooling, followed by a process of pelletisation. The pellets are subsequently dried and stored for future utilisation.

During the extrusion process, the masterbatch and base resin are dosed, mixed, and melted to form a continuous coloured encapsulant foil. The translucency of the foil can be adjusted by varying its thickness or the concentration of the colour masterbatch used in film production.

Extrusion represents a high-volume manufacturing process that is compatible with a variety of pigment types, encompassing both inorganic and organic categories. The process is typically operated at temperatures between 170°C and 200°C, allowing for the use of pigments with relaxed thermal stability constraints. In contrast, Digital Ceramic Printing (DCP) inks must withstand firing temperatures in excess of 500°C, which limits the choice of suitable pigments.

Interferential pigments, such as those offered by Merck or BASF, can produce coloured encapsulant, altering light reflection to create brilliant interference colours with performance losses below 20% in PV modules. However, these pigments exhibit higher colour angular sensitivity compared to absorbing pigments. Luminescent dyes are also compatible with extrusion and can be incorporated into coloured encapsulant formulations [31].

Coloured encapsulant can demonstrate high resistance to UV radiation, influenced by factors like pigments, additives, base resin, and environmental conditions. For instance, titanium dioxide pigmented foil may darken quickly under anaerobic conditions but remains stable in the presence of oxygen.

Figure 3.2-3 Freesuns project in Ferlens, Switzerland, with different tones of terracotta solar tiles.

Freesuns, a Swiss BIPV company, specializes in solar tiles that seamlessly integrate into buildings, including heritage roofs, in various colours. These tiles contribute to preserving traditional building aesthetics (see Figure 3.2-3). Solaxess, with a new generation of products, is currently commercializing coloured encapsulant films for BIPV applications. These coloured polymeric foils, laminated inside PV modules, create the desired appearance, as demonstrated in installations shown in Figure 3.2-4 [32].

Vanceva [33] and Trosifol [34] products are coloured encapsulant interlayers based on Polyvinyl butyral (PVB). PVB is commonly used in laminated safety glass for architectural applications, and it is also commonly used to laminate thin film modules.

Instead of applying the colour to the front encapsulant, the colour can also be implemented by adding an extra film with a colour print on it. This is generally applied in between two layers of encapsulant. It offers some extra flexibility with respect to the optimization of both colour and efficiency. An example is given in **Error! Reference source not found.**c.

Figure 3.2-4 BIPV building in Zürich made with a Solaxess [32] film and implemented by 3S Swiss Solar Solutions AG [89].

In this approach an additional film is inserted in the module stack between the cells and the front side material. This is often done by inserting the film between two encapsulant layers. The approach thus leads to additional materials. The colour is printed using standard offset printing techniques that give nice homogeneous colours and are very reproducible. By applying the film in front of the cells, the inhomogeneity of the cell appearance is filtered out. The drawback is that the film is often semi-transparent and thus the dark colour of the underneath cells is influencing the final colour appearance.

All these approaches do not rely on interference and show nice angular colour stability.

3.2.4 Colouring the front material

Finally, the colour can be applied to the front glass. This can be done either on the interior surface of the front material (glass or polymer-based) or on the exterior surface. The application of colour to the interior surface of the front material offers distinct advantages in terms of colour stability, as it provides enhanced protection against UV radiation. This is particularly beneficial in cases where the front material possesses inherent UV-blocking properties. This consideration assumes particular significance in the context of organic pigments. There are several methods by which colour can be applied to glass. These include the application of a multi-layer interference coating on glass or an organic or inorganic print on the glass. An illustrative example is presented in **Error! Reference source not found.**d.

Table 3.2-1 gives a non-extensive overview of the various colouring options and their respective manufacturers.

Table 3.2-1 Non-extensive overview of suppliers of coloured PV solutions.

Material	Coloring technology	Product name	Company
Cells	Cell coating (anti-reflection coating tuning)		LOF [35]
		Royal Glam /Mystic	Kameleon Solar [36]
Glass	Colored glass	BISOL Spectrum	BISOL [37]
		Silk color /Silk pro color	FuturaSun [38]
	Photonic pigment on either cell, foil or glass	ColorQuant™ Solar Technology	Merck [39]
	Mineral coating on glass (pigmented ceramic nanoparticles)	Suncol BAPV	SUNAGE [40]
	Multi-layer coating on glass (interference filter)	Kromatix	SwissInso [41]
			Emirates Insolaire [42]
			Kameleon Solar [43]
	Ceramic ink deposited (digital print hexagonal pixeled pattern) and hardened on glass (outside)	ColorBlast	Kameleon Solar [44]
	Ceramic printed dots, colored PVB foil, colored glass, coated cells		Ertex Solar [45]
	Anorganic pigments, print, ceramic color technic	solarix color	Solarix [46]
	Screen print on front glass	Desing2Power®	ISSOL (CSEM) [47]
	Print on glass (for Kameleon Solar)		Steinfort Glas (partner Kameleon Solar) [48]
PV material	Intrinsic property of dye solar cells (color depends on various factors such as electrolyte, substrate, concentration of the dye, etc.)		Solaronix [49]
	Intrinsic property of organic PV	HeliaSol / Heliafilm	Heliatek [50]
		ASCA films	ASCA (formerly OPVIUS + Amor) [51]
Encapsulant	Colored encapsulant (PVB)		Onyx Solar [52]
Interlayer	Nanotechnology-based interlayer	Solaxess	CSEM [53]
	Printed image on interlayer	Kaleo	CSEM [54]
	Printed foil laminated in (colored dots)	Solar Visuals	Solar Visuals [55]
		Sun Ewat Design	AGC (partner SolarVisuals) [56]
Foil	Printed foil		Sistine [57]
Thin film on glass	Multi-layer coating on glass (interference filter)	SKALA	Avancis GmbH [58]

The colour homogeneity of these technologies is generally satisfactory. In most cases, the cells behind are not visible anymore, and the colour itself is also nicely homogeneous.

However, in instances where the colour is derived from a multi-layer coating, angular homogeneity may be compromised. Nevertheless, there are notable exceptions, such as the works of Kromatix, which demonstrate the attainment of substantial angular colour stability (refer to Figure 3.2-5).

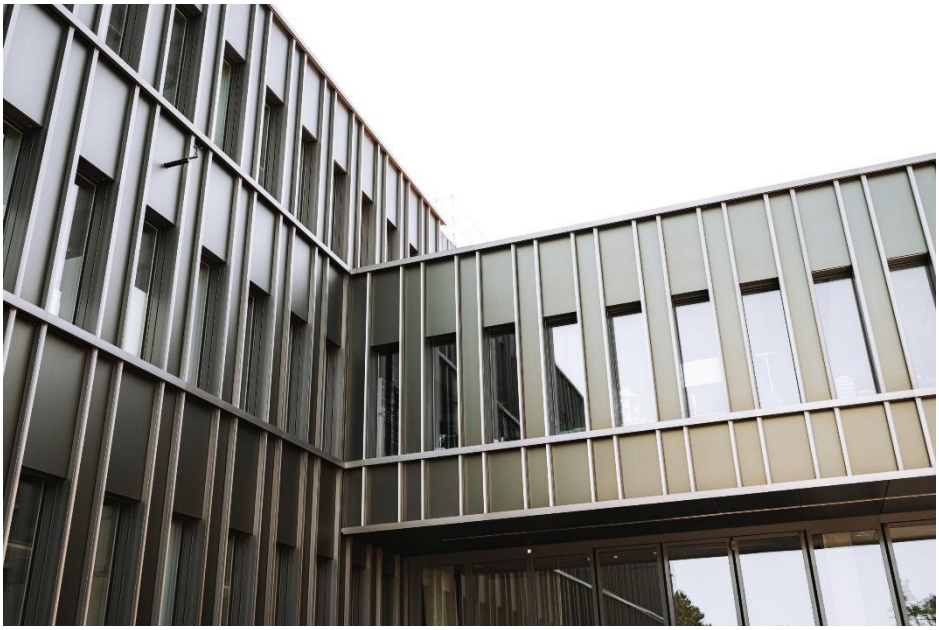

Figure 3.2-5 Example of angular colour stability of Kromatix panels.

3.2.5 Colour reproducibility

A precise and reproducible characterization of color is essential for colored Vehicle Integrated Photovoltaic (VIPV) products as a means of quality control during manufacturing and to evaluate the long-term stability of color solutions. Presently, there is a conspicuous absence of equipment capable of accurately characterizing the color of a surface situated behind a transparent layer, such as in a solar PV laminate. Typically, both academia and industry use conventional characterization methods using devices such as colorimeters and spectrometers based on integrating spheres to assess color. However, these conventional tools encounter a signal decrease when the sample being characterized is positioned behind a transparent medium like glass, leading to inaccurate color determination. In addressing this challenge, Borja Block et al. have proposed a novel colorimeter configuration, comprising a fiber optic spectrometer positioned at a 45° angle relative to the samples and utilizing a consistent and stable D65 light source. This innovative design enables precise colorimetric measurements under glass laminates [59]. The reproducibility and precision of color measurement ensure consistent quality in production and validate changes in color during long-term outdoor exposure. Presently, the evaluation of color is predominantly limited to a visual comparison against a reference RAL color palette.

Figure 3.2-6 Example of colour reproducibility of Kromatix™ Blue Green. Small colour differences can be observed. It does give the façade a more natural look.

Figure 3.2-7 Example of colour reproducibility of SolarVisuals. No colour differences can be observed.

3.2.6 Specific (RAL) colours

In many cases in the BIPV context, but certainly also in the VIPV context, customers request a specific (RAL) color. Most of the manufacturers mention customers demand colors. For instance, Kameleon Solar asserts its capacity to deliver customized RAL colors for its ColorBlast product. However, the cost associated with producing a full RAL panel for the colored film within the module is often deemed to be financially prohibitive. Inkjet printing offers greater flexibility, as evidenced by its applications in ceramic printing [60] or perovskite printing [61]. However, concerns regarding the long-term stability of the color remain.

4 WEIGHT

The weight of onboard photovoltaic (PV) systems is a critical factor to consider when integrating them into electric vehicles (EVs). This consideration arises from the fact that the PV system is in constant motion, necessitating additional energy. Consequently, it is imperative to account for this factor when evaluating the energy benefits of PV-powered vehicles. Although the weight of the onboard PV system is relatively small compared to the overall weight of an electric vehicle, and the power generated by the onboard PV is minimal in comparison to the power required to propel the vehicle, the weight and power characteristics of the onboard PV system differ significantly from those of the vehicle itself. Therefore, the weight of the PV system can substantially influence the overall performance and efficiency of the vehicle. It is thus essential to meticulously consider the weight and design of the onboard PV system when integrating it into a vehicle.

The pertinent question is whether the additional weight and power generated by the vehicle-integrated PV (VIPV) system positively impact the energy balance of EVs. The benefits are deemed positive if the energy produced by the PV system surpasses the additional energy consumed due to its weight. However, this assessment is not straightforward and is contingent upon the specific use case scenario. For instance, during parking, the additional energy demand attributable to the weight of the PV system is negligible, and the PV system can generate energy to support the charging of the EV's battery. Conversely, during driving at very low solar irradiance, such as at night, the PV system does not produce significant power, even though it necessitates an additional battery charge to move.

This section will examine the impact of PV weight in PV-powered vehicles for specific use case scenarios. Initially, the methodology will be presented, followed by the results of applying this methodology to two types of passenger vehicles. A comparison of the specific weight and performance of different PV technologies will also be conducted.

4.1 Influence of PV weight in PV-powered passenger vehicles

The methodology to evaluate how the energy balance of vehicles is affected by the additional weight of PV is presented by Patel et al. [62]. This method merges two simulation tools: the Future Automotive Systems Technology Simulator (FASTSim) [63] and PVWatts [64]. FASTSim computes the energy consumption of electric vehicles (EVs), while the PVWatts model calculates the PV energy yield. The flow of calculations done to assess the impact of weight on the energy balance of electric vehicles is shown in Figure 4.1-1. These simulations are performed to calculate an onboard PV yield factor, shown in Equation (1), to determine whether the net energy gain from onboard PV is positive or negative. A positive yield factor indicates a net energy gain, while a negative yield factor shows a net energy loss due to the onboard PV system. The yield factor is computed for a set of trips conducted over a period, such as a few months, using the mean values of energy yields and additional consumptions.

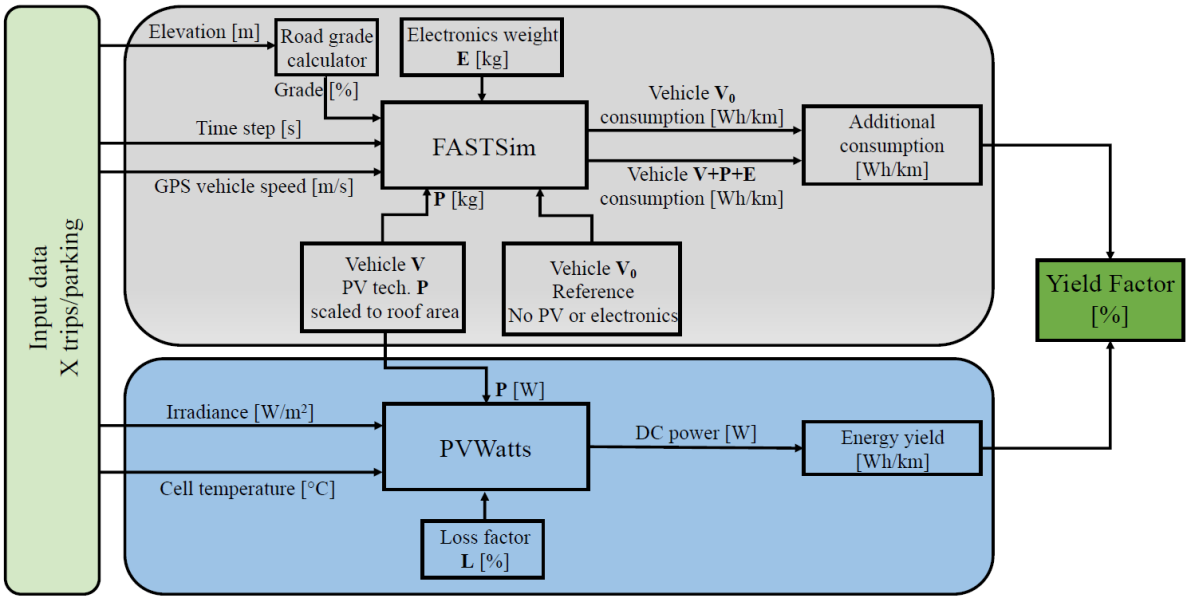

Figure 4.1-1 Representation of the data flow and calculations executed to determine the yield factors for various scenarios. Various inputs and outputs are marked with their respective units. X, P, V, V0, L, and E represent the variables changed in a loop to execute simulations for all scenarios mentioned. X is the individual trip/parking, P represents different PV technologies, V represents considered vehicles, V0 is the vehicle in reference configuration, L is the PV system loss factor with values of 5, 25, and 40%, E is the electronics weight with values of 1, 2.5, 5 kg.

$$F_{\mathrm{y}} = \frac{E_{\mathrm{y}} - \Delta E_a}{E_{\mathrm{y}}} \times 100, \tag{1}$$

where F_{y} is the onboard PV yield factor (%), E_{y} the energy yield (Wh/km), and $\Delta \mathrm{E}_a$ the additional consumption (Wh/km).

Equation (1) is used to calculate the yield factor during the driving phase of the vehicle. Calculating the yield factor during parking is necessary since parking time is also part of operating a vehicle with onboard PV. During parking, the vehicle has no additional consumption due to the PV weight and receives a positive energy yield during the daytime. Assuming the yield factor during the parking phase as (1), we introduce the total yield factor as a simple weighted sum of the driving and parking phases, as shown in Equation (2). It is important to note that since there is no additional consumption or energy yield during night-time parking, it is not considered part of the operation and is excluded from the total time.

$$F_{\mathrm{yt}} = F_{\mathrm{yd}} \times \frac{t_{\mathrm{d}}}{t_{\mathrm{t}}} + \left((1 - \frac{t_{\mathrm{d}}}{t_{\mathrm{t}}}) \times 100 \right), \tag{2}$$

where F_{yt} is the total yield factor (%), F_{yd} the driving phase yield factor (%), and $\frac{t_{\mathrm{d}}}{t_{\mathrm{t}}}$ the driving fraction of the total time.

The power required to propel an electric vehicle at any given moment is the sum of the power demands of its subsystems and the physical forces it must overcome. This is shown in Equation (3).

$$P_T = \underbrace{P_{\mathrm{w}} + P_{\mathrm{d}} + P_{\mathrm{x}}}_{\text{Weight independent}} + \underbrace{P_{\mathrm{a}} + P_{\mathrm{s}} + P_{\mathrm{r}} - P_{\mathrm{b}}}_{\text{Weight dependent}}, \tag{3}$$

where P_T is the total power demand (W), P_w the power to overcome rotational inertia of wheels and transmission (W), P_d the power to overcome wind drag (W), P_x the auxiliary power consumption (W), P_a the acceleration power needed (W), P_s the power to overcome road slope (grade) (W), P_r the power to overcome tire rolling resistance (W), and P_b the regenerative braking power (W).

The power needed for acceleration, overcoming road slope, overcoming tire rolling resistance and regenerative braking are all weight dependent. The total power demand is simulated using the Python version of FASTSim. The drive cycle, comprising timestep, vehicle speed, and road grade, is one of the input variables FASTSim requires to execute energy consumption simulations for different vehicle types. Road grade is calculated outside of FASTSim using the method adapted from [65], which involves smoothing GPS elevation data and taking the differential between consecutive GPS points of a trajectory. Vehicle specifications like curb weight, drag coefficient, frontal area, battery, motor capacities, and efficiencies are taken directly from the FASTSim database and used without modifications. Vehicle speed and road grade values are the two most important variables influencing a vehicle's additional energy consumption due to added weight. FASTSim is used to simulate two configurations, reference and VIPV, using a set of drive cycles derived from measurement data, described in the following section, to calculate the additional energy consumption. Depending on the PV technology used, the additional weight of the onboard PV system is directly added to the curb weight of the considered vehicles. The reference configuration represents no added PV or control electronics weight, and its energy consumption numbers will be subtracted from the VIPV configuration to calculate the additional consumption.

The PVLIB-Python [66], version 0.9.3, implements the PVWatts model [64] to calculate the energy yield of the onboard PV system. This model generates an electrical power time series in W that the PV system can produce for a specific drive cycle. We measure this power generation and divide it by the distance of that particular drive cycle to determine the energy yield of the PV system in Wh/km. To calculate the PV system's DC power generation, the PVWatts model requires the following input: plane-of-array (POA) irradiance (W/m^2), cell temperature (°C), module power at STC (W), and temperature coefficient of power (%/°C). The model considers various system losses using a total system loss factor [64]. For onboard PV applications, mismatch, wiring, parasitic consumption, and curvature losses are the primary contributors to the total system loss factor. However, it is challenging to determine concrete system loss factors for onboard PV because only a little measurement data has been published. In this study, we assume a range of values for the loss factor, which are 5%, 25%, and 40%. It is essential to note that the shading loss is not deducted as a loss factor but is already incorporated into the measured POA irradiance used to calculate the yield.

4.2 Case study

The case study we conducted examines several PV technologies, including PERC, IBC, SHJ, CdTe, and CIGS. These technologies have a specific power range of 148 to 249 W/m^2, as shown in Table 4.2-1, and their efficiency ranges from 14.8 to 24.9%, with PERC, IBC, and SHJ being the dominant silicon technologies. The specific weight in kg/m^2 is scaled to the roof size of the considered vehicles. It is essential to note that the specific weights of VIPV technologies consist only of the weight of the PV active material, including cell material, interconnects, and a single layer of encapsulant (Ethylene-Vinyl Acetate, EVA) weighing about 150 gm/m^2. The weights of active materials of different PV technologies and the encapsulant are taken from Reese et al. [67]. We assume that the PV cells are sandwiched between the

vehicle roof glass sheets at the back and front sides to provide structural and mechanical durability to PV cells and protection against humidity. To calculate the energy yield of the considered PV technologies, we use the specific power in W/m^2 scaled to the roof size of the vehicles. Although it is challenging to find commercial offerings for the control electronics to track the onboard PV output and feed it into the high-voltage traction battery, we assume their weight based on the generic ones available for the automotive sector. For instance, a DC-DC converter for an automotive application can weigh around 2.5 kg, as seen in some examples [68] [69]. These converters are usually rated in the ranges of several kW, and onboard PV for passenger cars will likely be in the range of a few hundred to a thousand watts. Therefore, the assumed control electronics weight in this study could be an overestimation for most cases. To address this uncertainty, we assume the weight of the control electronics consisting of MPPT, DC-DC converters, and wiring as three scenarios of 1, 2.5, and 5 kg.

Simulations in this study utilize the 2016 Nissan Leaf and 2016 Tesla Model S electric vehicles based on specifications from the FASTSim database.

Table 4.2-1 List of PV technologies and their specific weight, power, and temperature coefficients of power. Weights are specified for VAPV and VIPV configurations separately. The sources of each value are indicated in the brackets. Sources for STC efficiency are same as STC specific power.

PV technology	VIPV weight [kg/m^2]	STC Specific power [W/m^2]	STC Efficiency [%]	Temperature coefficient of power [%/°C]
PERC	0.80 [67]	173 [70]	17.3	-0.40 [70]
IBC	0.80 [67]	177 [71]	17.7	-0.35 [71]
SHJ	0.80 [67]	190 [72]	19.3	-0.32 [72]
CdTe	0.19 [67]	190 [73]	19.0	-0.32 [73]
GaAs	0.20 [67]	249 [74]	24.9	-0.09 [74]
CIGS	0.19 [67]	148 [75]	14.8	-0.36 [76]

It is assumed that the onboard PV is situated exclusively on the roof area of each vehicle, with the Leaf having 1.8 m^2 of roof area while the Tesla Model S has 2.5 m^2 of roof area [4]. The data used to derive the drive cycles needed for the FASTSim simulations is based on measurement campaigns [77] [78] conducted in 2021 in Germany's Jülich and Hannover regions. The variables considered in this study include timestamps (in seconds), GPS vehicle speed (in meters per second), GPS elevation (in meters), roof irradiance (in watts per square meter), and roof cell temperature (in degrees Celsius). The datasets have an average measurement frequency of 0.5-1 Hz and were collected between March and October 2021. Two hundred sixty completed trips, covering a distance of 5 840 km, have been analyzed. The trips were mostly taken during the day between 6:00 and 19:00 local time.

4.3 Results

We have generated simulation outcomes for specific parameters detailed in the above section. The parameters include two electric cars equipped with different PV technologies in integrated configuration. We have taken into account different electronics weights and system loss factors. Using FASTSim, we have simulated the additional consumption in Wh/km attributed to the onboard PV weight. The additional consumption is calculated by comparing the consumption of a reference case (without onboard PV) to the consumption with various onboard PV scenarios. The results are presented in Figure 4.3-1, which shows the additional energy consumption of individual trips attributable to respective PV system weights. We present boxplots representing the considered PV technologies in the VIPV configuration for the 260 trips.

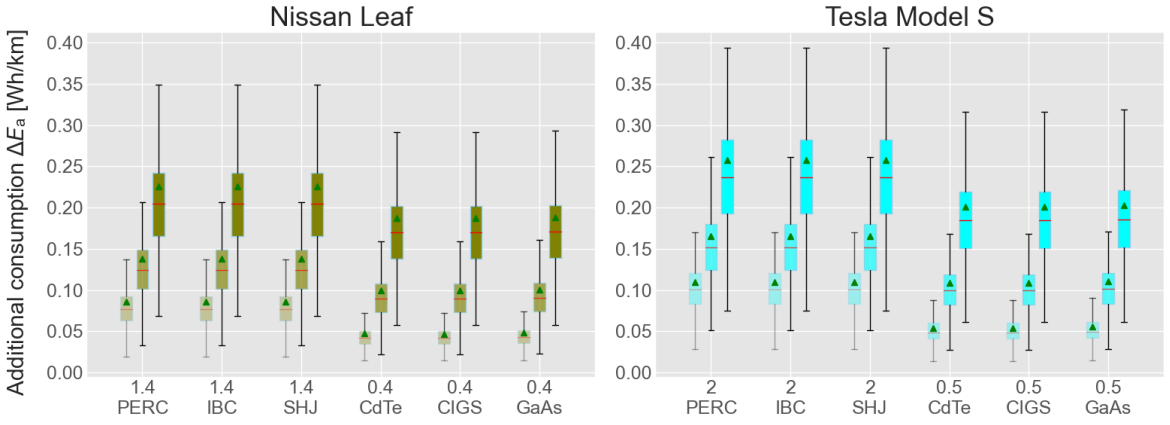

Figure 4.3-1 Additional consumption for VIPV configuration in Wh/km. The PV technologies considered are shown with the weight of each system in kg scaled to the respective car roof area. On top of the PV weight, three different electronics weights are added for each technology which can be seen as three separate boxplots. The lighter shade represents an electronics weight of 1 kg, the medium shade is 2.5 kg, and the darker shade is 5 kg.

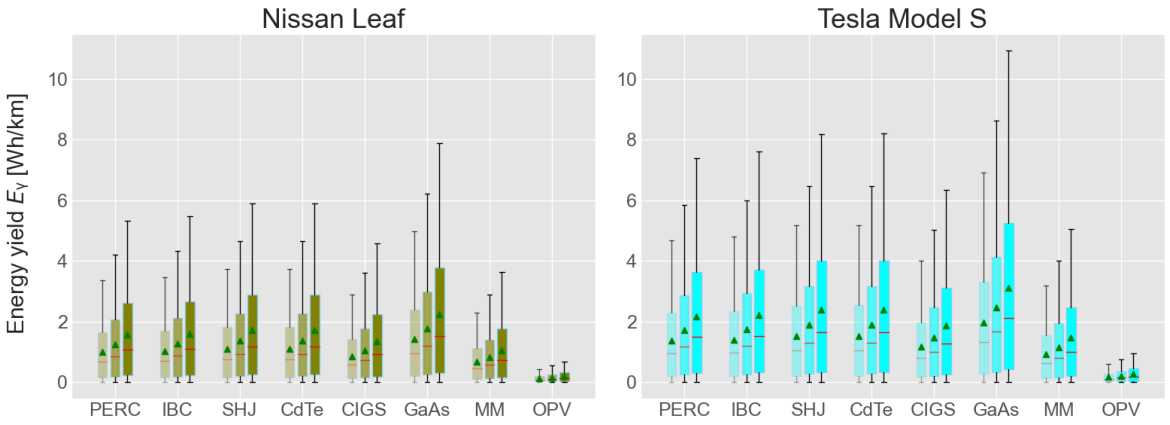

Figure 4.3-2 Energy yield for different PV technologies in Wh/km. The lighter shade represents a loss factor of 40%, the medium shade is 25%, and the darker shade is 5%.

The variations in the box plot for each technology are due to the different vehicle speeds and driving terrain for the simulated trips. The additional consumption is in the average range of 0.05 to 0.26 Wh/km.

We have calculated the energy yields for the different PV technologies using the PVWatts model, as shown in Figure 4.3-2. Three boxplots for each PV technology represent variations in the assumed system loss factors. The variations in energy yields of each PV technology are because the irradiance measurements for these trips were carried out for different times of day, weather, and surroundings. The energy yields during the trips are converted to Wh/km for uniform comparison with additional consumption.

The average energy yields for the considered PV technologies range from 0.12 to 3.12 Wh/km. Some boxplot values are close to zero, representing driving scenarios during early morning and late evening when the available irradiance is low. By using the simulated additional consumption and energy yields, we have calculated the yield factor to determine the impact of the weight of each PV technology. A yield factor of 100% would indicate that the onboard PV weight has zero impact on the vehicle's energy balance. A yield factor of 0% indicates that the total energy yield compensates for the consumption attributable to additional weight. A negative yield factor suggests that the car consumes more additional energy than it can generate due to the onboard PV. We have calculated the yield factor for each PV technology using the results shown in Figure 4.3-1 and Figure 4.3-2 for nine combinations of assumed electronics weight and system loss factors. We have used the mean values for each PV technology in the boxplots of Figure 4.3-1 and Figure 4.3-2 to avoid skewed yield factors for cases when the energy yield for the trips that occur very early in the morning or late evening have close to zero value. The yield factors for the nine combinations of electronics weights and loss factors are shown as a heatmap in Figure 4.3-3.

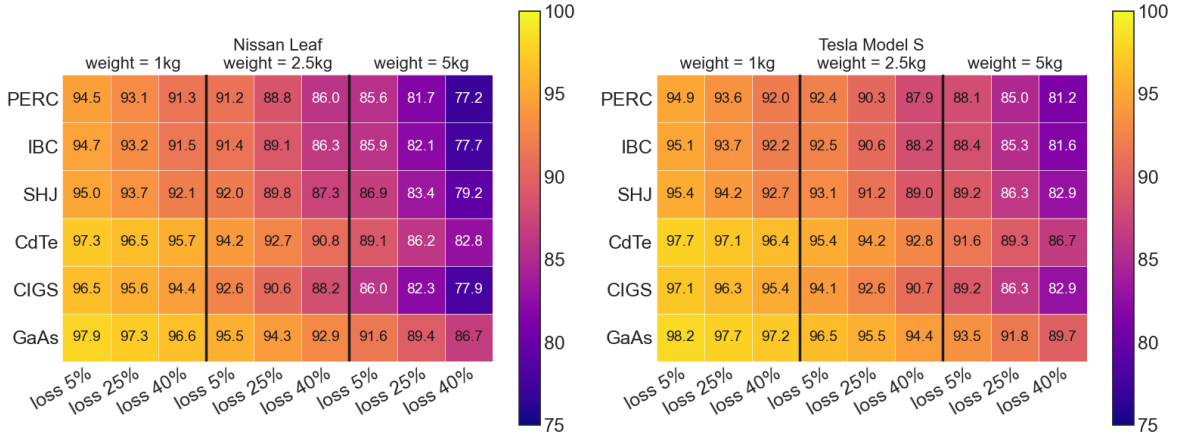

Figure 4.3-3 Yield factors for VIPV configuration. The heatmap represents yield factors for nine combinations of electronics weight and system loss factors for 6 VIPV technologies. The VIPV weights are the same as in Figure 4.3-1. The columns are broadly divided according to electronics weight ranges of 1, 2.5, and 5 kg, each representing 5, 25, and 40% loss factors. The best-case scenario is on the left of the respective figures with an electronics weight of 1kg and a loss factor of 5%. The worst-case scenario is on the right, with an electronics weight of 5 kg and a loss factor of 40%.

For VIPV technologies, the yield factors are in the 77.2% to 89.7% range in the worst-case scenario and 94.5% to 98.2% range in the best-case scenario for both vehicles combined. The yield factors we presented only consider the driving phase and do not consider the parking

state. Although our simulations only cover a limited set of trips for two specific electric vehicles and are unsuitable to provide a concrete evaluation of PV technologies' weight, they demonstrate that the impact of PV weight for onboard applications is significant if energy yield during the parking phase is not considered. This methodology can use comprehensive trip and parking state data to determine which technology is more appropriate for onboard PV applications from a weight perspective.

5 COMPLIANCE AND SAFETY

As an integrated application of photovoltaics, vehicle integrated PV needs to comply with the safety norms of photovoltaics as well as automotive. Currently, there is no standard for physical integration of VIPV, just independent standards for automotive industry and solar panels. Final acceptance of vehicles (with or without VIPV) will be given by local road authorities according to their own test protocols. Furthermore, the special PV application in vehicles requires PV performance tests to be adopted, due to module curvature and highly dynamic response as compared to stationary PV systems.

This chapter summarizes the progress and recommendations in this field.

5.1 Overview of testing standards for PV and automotive sectors

There is not yet a dedicated standard for vehicle integrated PV (VIPV). However, in a joined publication of November 2021 by Fraunhofer ISE from Germany and TNO from the Netherlands, a proposal has been made for a safety qualification program for VIPV. [79] In this proposal, the authors start from the standard test requirements for newly developed PV modules, IEC 61730-2:2016 which describes the guidelines for safety qualification of conventional PV modules. This standard is then compared to the ISO 16750 that describes environmental stress and tests and requirements for electronic components in vehicles. There is a large overlap in test requirements between these two standards. Some are more stringent in the IEC 61730, others in the ISO 16750. Besides these two standards, there are additional standards in automotive that play a role for VIPV. Table 5.1-1 gives an overview of the standards that were considered as important for VIPV and taken into account in the proposal.

Table 5.1-1 Overview of the standards considered as important for VIPV

Standard	Description
ISO 16750	Road vehicles Environmental conditions and testing for electrical and electronic equipment
ISO 20653	Road vehicles Degrees of protection (IP code) Protection of electrical equipment against foreign objects, water and access
ECE-R10	Automotive electromagnetic compatibility (EMC) testing
ECE-R43	Uniform provisions concerning the approval of safety glazing materials and their installation on vehicles
ECE-R95	Uniform provisions Concerning the Approval of Vehicles with regard to the protection of the occupants in the event of a lateral collision
ECE-R100	Uniform Provisions Concerning the Approval of Vehicles with Regard to Specific Requirements for the Electric Power Train
ECE-R118	Uniform technical prescriptions concerning the burning behavior of materials used in the interior construction of certain categories of motor vehicles

ECE-R127	Uniform provisions concerning the approval of motor vehicles with regard to their pedestrian safety performance

In ISO 16750-1 pass criteria are given by functionality classes. The authors find classification of a VIPV module according to those functionality classes insufficient and suggest using the pass criteria from IEC 61730:2016 to ensure safe operation of the VIPV modules in terms of electrical functionality and mechanical design.

In this proposed safety qualification program, a few tests are removed with respect to the original IEC61730-2. The Fire Test (MST 23) can be removed if there is a guarantee that flammable splinters will not penetrate to the passenger compartment. In that case, the fire resistance specifications of IEC 61730-2 are sufficient. The Module Breakage Test (MST 32) can be replaced by the phantom fall test with its more stringent pass criteria.

Then there are a few suggestions for additional tests on the VIPV module compared to the IEC61730-2. These are the Ball-drop Test (ECE-R43) which is a requirement to ensure rupture safety. As mentioned above, the Phantom Fall Test (ECE-R43) with a complete module is required as a replacement of the Module Breakage Test (MST32), and the Headform Test (ECE-R127) for bonnets needs to be added in view of pedestrian safety.

Sequence D of the IEC61730-2 has a parallel branch next to the Damp Heat test and mechanical load test. Here an additional Vibration Test IV or V from ISO 16750-3 should be performed to ensure mechanical stability under vibrations resulting from e.g. door slamming or rough road driving. For this reason, also a Mechanical shock Test form ISO 16750-3 is added here.

Also, a sequence E1 is added with Chemical Resistance Tests (ISO 16750-5) ensuring module stability against chemical loads and a Salt Mist Corrosion Testing (IEC 61701 and IEC 60068-2-52) for ensuring the environmental stability of modules in winter.

In sequence F an addition Vibrational Test IV or V (ISO 16750-3) is inserted between the Temperature Test (MST21) and the Hot-Spot endurance test (MST22). Previous observations suggest that vibrational loads, as they are expected during VIPV operation, increase the probability of crack formation and/or propagation in solar cells. Consequently, the risk of hot-spot formation, which might exceed the worst-case scenario examined throughout the hot-spot test according to IEC 61730-2:2016,

An additional sequence H is dedicated to additional climatic tests. For glass containing parts this concerns Increased Temperature (A3/5), Irradiation Resistance (A3/7) and Humidity Resistance (A3/8) testing. For polymers the Cross-cut Test (A3/13), Humidity Resistance test (A14/6.4 or A16/6.4) and Weathering Resistance (A3/6.4) should be performed. This stems from the Climatic testing for safety glass. Part of these tests require more stringent requirements than the IEC 61730-2:2016.

Finally, the proposed qualification program suggests making 3 test voluntary. Namely Cut Susceptibility test MST12, Gravel Bombardment test from ISO 16750- and hail test MQT 17 IEC61215-2. These are not related to safety. However, by adding these tests, the robustness of the VIPV panels against these impacts provides a better guarantee for the durability of the visual appearance.

Since the appearance of the paper, in 2023 an updated version of IEC 61730-2:2016 was published. From the significant revisions, the following are relevant in view of the VIPV qualification program:

- MST 21: Temperature test has been removed from this standard because modules tested individually in unrestricted mounting systems in open-air climates below 40 °C operate at or below a 98th-percentile operating temperature of 70 °C. As a result, the existing IEC 61730-1 requirement for a minimum RTI/RTE/TI of 90 °C is adequate. To address modules operating at higher temperatures, IEC TS 63126 includes an informative annex to describe tests and analysis techniques suitable for estimating the 98th-percentile operating temperature. This covers system effects such as mounting methods that restrict airflow and result in a 98th-percentile module operating temperature in excess of 70 °C.
- MST 32: Module breakage test is no longer required for Class 0 modules. As this test is replaced by the Phantom Test in the proposed qualification program, this is not relevant. Besides class 0 modules are only used in restricted areas which is not the case for VIPV.
- MST 54: Instead of sequential test with one module, now one module for sequence B shall be irradiated from the front side and another module from the backside during the 60 kWh/m2 cycle. *Conditions were already harsher and have been increased even further so new MST54 should be used.*
- MST 57: Evaluation of insulation coordination added. The purpose of this test is to evaluate if the minimum clearances and creepage distances, distances through cemented joints as well as distance through functional insulation given in Tables 3 and 4 of IEC 61730-1:2022 are met. For distances inside a junction box, after installation and termination of ribbons, the minimum values of IEC 62790 have to be met. This is also relevant for VIPV and should be added to the test sequence.
- All MQT references updated to revised IEC 61215 series Ed.2.0 2021. Where MQT test are described in the proposed safety qualification program, the updated versions should be used.
- Bifacial modules: Requirements updated for MST 02 Performance at STC, MST 07 Bypass diode functionality test, MST 22 Hot-spot endurance test, MST 25 Bypass diode thermal test and MST 51 Thermal cycling (TC200). For now, bifacial modules will probably not be part of VIPV products. Otherwise, these updates should be followed.

The PV technology – and in particular VIPV – is a fast-developing technology. The adoption of the safety and quality tests required for different national road authorities needs to catch up and harmonize to enable a better market penetration of VIPV.

5.2 Testing examples of different PV technologies

In general, photovoltaic (PV) modules are subjected to testing to evaluate their suitability for use in vehicle exterior and electrical components. Typical environmental tests for PV products were conducted to examine long-term (typically 25 years) degradation. Conversely, the objective of automotive-components testing is to identify defects that arise from exposure to harsh environments and mechanical stresses, while maintaining the fundamental functionality of the components. The number of testing items is more significant, but the testing durations are less. Typically, the successful completion of the module's environmental tests for PV devices is indicative of its ability to pass vehicle-related tests. However, it is necessary to confirm this by the standard tests for automotive exterior and electronics, depending on the relatively weak performance of PV devices at high temperatures and cycles.

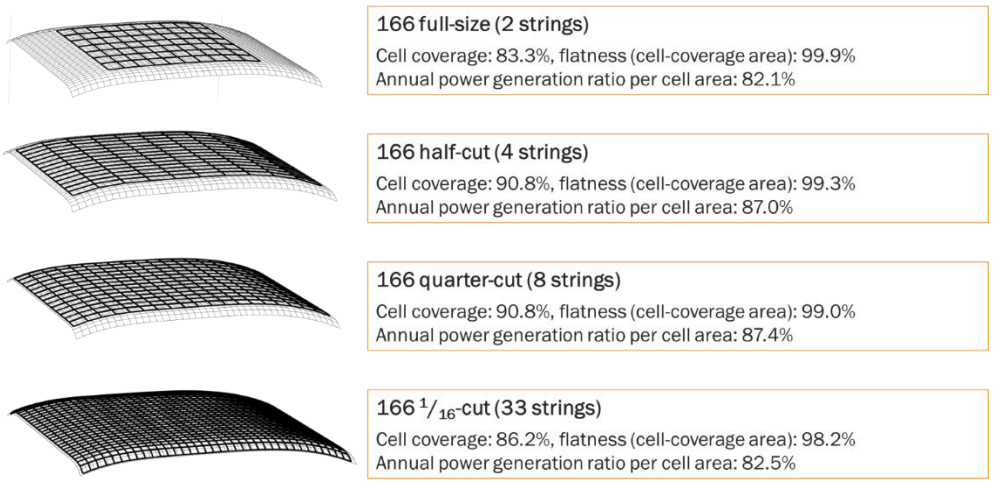

Figure 5.2-2 Performance of PV devices on the curved surface: coverage and losses on a curved surface [90] examined by the representative curved surface (set of the median values of the curve parameter defined by [80].

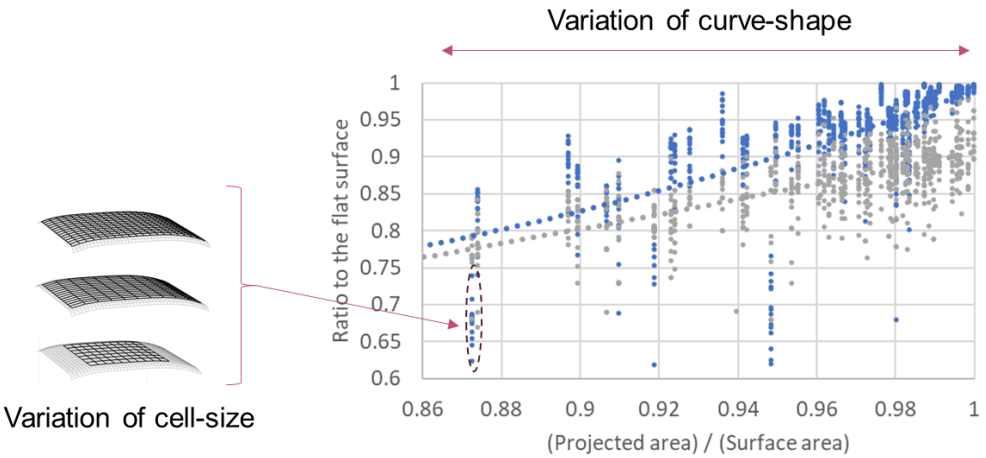

Figure 5.2-1 Ratio of energy yield by the curve-shape [92]. The energy yield is affected by the shading zone and latitude. Calculated by (61 curved surfaces) X (14 cell sizes). The number of stings varies by cell size (ex., 2 for full-size and 33 for 166 1/16 cut).

Another concern for testing and designing that is specific to PV products for vehicles is that the behavior of PV devices is sensitive to curved shapes, as discussed in Section 2. The behaviors of these modules exhibit significant variation depending on the curve shape. In principle, it is essential to test every shape of the curved surface, considering its sensitivity to the curvature. However, a comprehensive study on the representative population of curved surfaces for vehicles will be beneficial [80] [81]. Utilizing a representative curved shape enables the estimation of the coverage ratio (c-Si cells) and facilitates the optimization of string configurations, as illustrated in Figure 5.2-1 and Figure 5.2-2.

5.3 Special testing requirements for curved PV

Most equations and measurement methods of solar cells and modules are based on the assumption that cells and modules are flat. Even the most straightforward equation, like (Power) = (Efficiency)×(Area)×(Irradiance), is not valid for curved cells and modules.

The minimum requirement for scientists and engineers dealing with curved solar cells and modules is to establish a reproducible testing method. For this purpose, we conducted international round-robin projects several times involving testing laboratories and research institutes. Nanjing AGG Energy, China, prepared the glass-covered rigid modules, including four levels of the radius of curvatures. Figure 5.3-1 shows the summary of the measured values by testing laboratories.

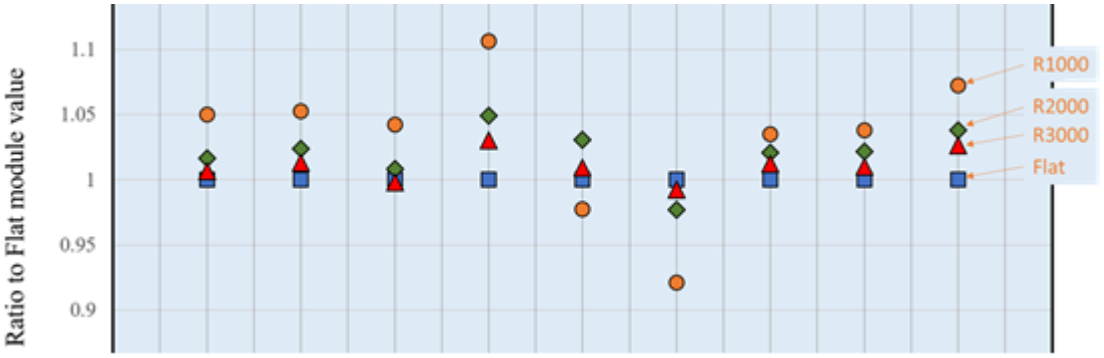

Figure 5.3-1 Test results by testing laboratories and research institutes (Blind test) [91].

The reproducibility of the curved module was hampered by the increase of curvature (decrease of radius of the curvature). However, we found a rule that the acceptance of the test result is constrained by the size of the module and the geographical conditions of the light source of the solar simulator (Figure 5.3-2). Currently, 19 testing laboratories and research institutes worldwide (11 countries) are confirming the testing protocol and acceptance rule by blind tests.

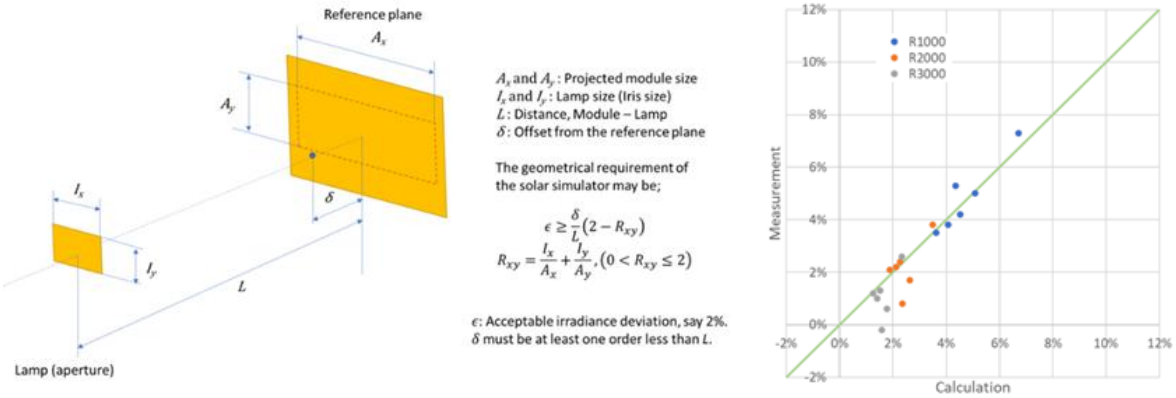

Figure 5.3-2 Acceptance criteria of the solar simulators for curved solar cells and modules [91].

The test method for curved modules targeted reproducible measurement and not always equivalent outdoor performance. This was examined using commercial VIPV (Vehicle-integrated PV) products for the curved roof of the Toyota Prius. For flat PV devices, (Indoor test) = (Outdoor operation), in principle. For the curved PV devices, (Indoor test) ≠ (Outdoor operation), inherently. The inherent mismatching loss appears outdoors due to variations of the cosine loss among solar cells. The loss in the curved module can be modeled by the vector computation based on differential geometry. (Figure 5.3-3, Figure 5.3-4).

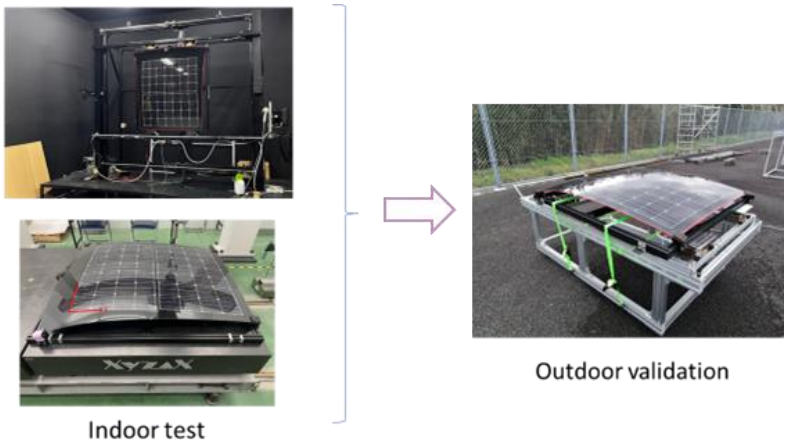

Figure 5.3-4 Outdoor test validation after indoor tests by testing laboratories satisfying the requirements for the curved PV devices shown in Figure 5.3-1. [87].

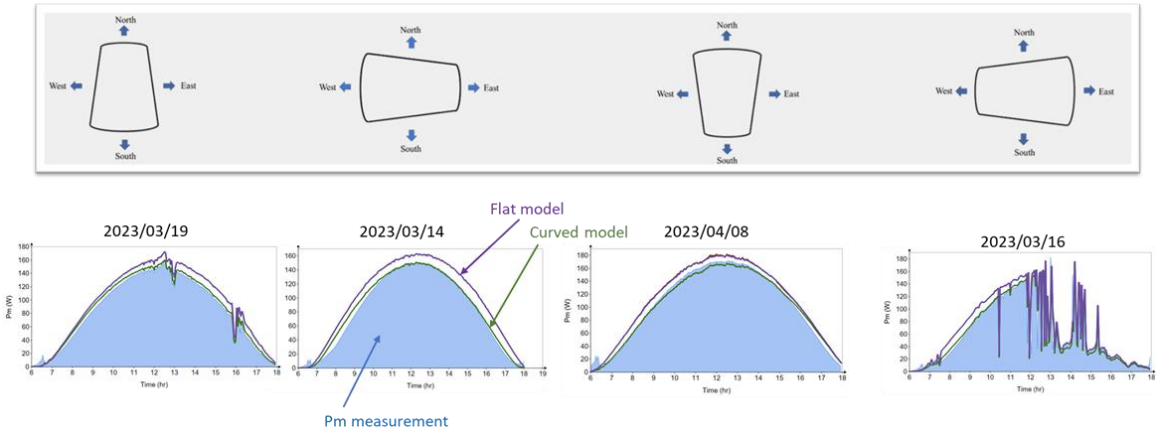

Figure 5.3-3 Outdoor test validation in various orientations – comparison to the actual performance and curve-correction calculation [91].

The development of a test method to evaluate the performance of a curved PV module is a first and essential step for performing yield estimations of the VIPV system. For stationary, flat PV systems, the performance data of the module, location, orientation, irradiance and weather data is sufficient for an annual yield calculation. In case of a VIPV system, the situation is much more complex. Along with the performance of the curved modules, information about the commute pattern, the charging strategy, battery size, dynamic shading, etc. is required. Currently, there is no standard protocol that allows comparing different VIPV systems with respect to their annual yield.

5.4 Toxic materials

VIPV systems may incorporate toxic materials, e.g. lead in perovskite-based solar modules. For the automotive sector, political regulations may exist, depending on the country, that clearly limit the incorporation of toxic materials. Furthermore, recyclability of any vehicle component might be subject of regulations as well. It's not the purpose of this document to research the current status of such regulations, but the technological considerations of VIPV, as regulations may be changed by policy.

5.5 Vibration robustness

Cell crack by vibration is a significant risk for the long-term reliability of photovoltaic modules. The standard design of the photovoltaic modules uses EVA as the cushion, shock absorber, and damping material of the vibration. EVA is known as the superior material for damping vibrations for structures. However, the damping performance is visible in the 0.1 Hz to 10 Hz region, where the vibration of architectural structures. On the contrary, the vibration of transportation and vehicle applications lies up to 1 000 Hz (trucks) and 2 000 Hz (passenger cars). In this region, EVA's molecular chain movement cannot catch up with the vibration speed, and its damping factor drops to less than 0.1, which is almost no help for damping vibration.

Cell cracking may be caused by resonance in a wide range (100 - 2 000 Hz) of vibrations at the roof surface of the car body. The natural resonance of the solar cells in the PV modules for vehicles can be avoided by the resonance design, typically by adjusting the tab ribbons. The test can be made by observing the coherency of the vibration caused by impact by an impulse hammer.

6 CONCLUSION

This report provides a comprehensive overview of vehicle-integrated photovoltaic (VIPV) systems, covering various aspects such as technology considerations, aesthetics, energy balance, compliance, and safety. The report discusses the challenges and opportunities associated with integrating PV systems into vehicles, including curvature considerations, coloring techniques, weight implications, and testing standards.

Key points from the document include:

- Curvature considerations for VIPV, including manufacturing techniques and impact on performance.
- Aesthetic aspects, such as coloring techniques and their impact on efficiency.
- Energy balance analysis, considering the additional weight of PV systems and their energy yield.
- Compliance and safety standards, combining requirements from both PV and automotive sectors.
- Special testing requirements for curved PV modules.

The document highlights the need for further research and development in areas such as:

- Optimizing PV cell and module designs for curved surfaces.
- Improving coloring techniques to balance aesthetics and efficiency.
- Enhancing energy yield while minimizing weight impact.
- Developing standardized testing protocols for VIPV systems.
- Addressing vibration robustness and potential issues with toxic materials.

Overall, the report emphasizes the potential of VIPV systems to contribute to sustainable transportation while acknowledging the technical challenges that need to be addressed for widespread adoption.

REFERENCES

[1] R. Bartolucci and A. Di Filippo, "Curved photovoltaic module and its production method". Patent EP1564816A1, 2005.

[2] R. Mangu, K. Prayaga, B. Nadimpally and S. Nicaise, "Design, Development and Optimization of Highly Efficient Solar Cars: Gato del Sol I-IV," *2010 IEEE Green Technologies Conference,* pp. 1-6, 2010.

[3] K. Araki, A. J. Carr, F. Chabuel, B. Commault, R. Derks, K. Ding, T. Duigou, N. J. Ekins-Daukes, J. Gaume, T. Hirota, O. Kanz, K. Komoto, B. K. Newman, R. Peibst, A. Reinders, E. Roman Medina, M. Sechilariu, L. Serra, A. Sierra, A. Valverde and D. Zurfluh, "State-of-the-Art and Expected Benefits of PV-Powered Vehicles," International Energy Agency, https://iea-pvps.org/key-topics/state-of-the-art-and-expected-benefits-of-pv-powered-vehicles/, 2021.

[4] M. Heinrich, C. Kutter, F. Basler, M. Mittag, L. E. Alanis, D. Eberlein, A. Schmid, C. Reise, T. Kroyer, D. H. Neuhaus and H. Wirth, "Potential and Challenges of Vehicle Integrated Photovoltaics for Passenger Cars," in *37th European PV Solar Energy Conference and Exhibition*, Lisbon, 2020.

[5] B. Commault, T. Duigou, V. Maneval, J. Gaume, F. Chabuel and E. Voroshazi, "Overview and Perspectives for Vehicle-Integrated Photovoltaics," *Appl. Sci.,* vol. 11, no. 24, p. 11589, 2021.

[6] H. Samadi, G. Ala, V. Lo Brano, P. Romano and F. Viola, "Investigation of Effective Factors on Vehicles Integrated Photovoltaic (VIPV) Performance: A Review," *World Electr. Veh. J.,* vol. 14, no. 6, p. 154, 2023.

[7] "How to Install Flexible Solar Panels for Car Roof," Sungold, [Online]. Available: https://www.sungoldsolar.com/how-to-install-flexible-solar-panels-for-car-roof/. [Accessed 22 12 2023].

[8] E. Bellini, "Vehicle-integrated solar kit may reduce frequency of recharging by 14%," pv magazine, [Online]. Available: https://www.pv-magazine-australia.com/2022/09/26/vehicle-integrated-solar-kit-may-reduce-frequency-of-recharging-by-14/. [Accessed 22 12 2023].

[9] "Solar cells in vehicles (VIPV): between research and realism," IMEC, [Online]. Available: https://www.imec-int.com/en/articles/solar-cells-vehicles-vipv-between-research-and-realism. [Accessed 22 12 2023].

[10] V. Rosca, N. Guillevin, L. A. G. Okel and B. K. Newman, "Prefab Approach to Mass Customization," in *SiliconPV Conferenz*, Konstanz, 2022.

[11] L. A. G. Okel, N. Guillevin, E. Hoek, O. Apaydin, V. Rosca and B. K. Newman, "Manufacturing high-yield, low-cost, lightweight VIPV components," in *PVinMotion*, 's-Hertogenbosch, 2023.

[12] B. K. Newman, "Advances in conductive back sheet module technology for emerging applications," in *Back Contact Workshop*, Munich, 2022.

[13] A. K. Shukla, K. Sudhakar and P. Baredar, "A comprehensive review on design of building integrated photovoltaic system," *Energy and Buildings,* vol. 128, pp. 99-110, 2016.

[14] B. P. Jelle and C. Breivik, "State-of-the-art Building Integrated Photovoltaics," *Energy Procedia,* vol. 20, pp. 68-77, 2012.

[15] B. P. Jelle and C. Breivik, "The path to the building integrated photovoltaics of tomorrow," *Energy Procedia,* vol. 20, pp. 78-87, 2012.

[16] B. Commault, B. Chambion, L. Serra, F. Karoui and S. Nassibi, "On-Board Photovoltaic Kit for Existing Vehicles," in *8th World Conference on Photovoltaic Energy Conversion*, Milano, 2022.

[17] B. Chambion, B. Commault, H. Robin, J. Gaume and S. Guillerez, "Flexible PV Module". Patent WO 2023/036663.

[18] T. Duigou, S. Caplet, B. Chambion and J. Gaume, "Numerical simulation and experimental characterization of c-Si cells mechanical limits in spherical curvature shape," in *38th EU PVSEC*, Lisbon, 2021.

[19] J.-H. Zhao, J. Tellkamp, V. Gupta and D. R. Edwards, "Experimental Evaluations of the Strength of Silicon Die by 3-Point-Bend Versus Ball-on-Ring Tests," *IEEE Transactions on Electronics Packaging Manufacturing,* vol. 32, pp. 248-255, 2009.

[20] Toyota, "Prius Plugin," [Online]. Available: https://www.toyota.ie/models/prius-plugin.

[21] "pv-manufacturing," [Online]. Available: https://pv-manufacturing.org/paved-pv-modules/.

[22] N. Roosloot, J. Zhu, S. E. Foss and G. Otnes, "Extended Thermal Cycling of Shingled Cell Interconnects," in *2021 IEEE 48th Photovoltaic Specialists Conference (PVSC)*, Fort Lauderdale, FL, USA, 2021.

[23] J. Lippiatt, S. Westerberg and D. Rose, "The Impact of a Faster Thermal Cycling Profile on PV Cell Interconnect Cycles to Failure," in *IEEE 7th World Conference on Photovoltaic Energy Conversion (WCPEC)*, Waikoloa, HI, USA, 2018.

[24] P. C. de Jong, "Achievements and challenges in crystalline silicon back-contact module technology," *Photovoltaics International 7th Edition,* pp. 138-144, 2010.

[25] B. de Gier , "Mass customization of back-contact PV modules," in *11th Back Contact Workshop*, Hameln, Germany, 2023.

[26] V. Rosca, N. Guillevin, L. A. G. Okel and B. K. Newman, "Prefab approach to mass customization of integrated PV," in *SiliconPV 2022*, Konstanz, Germany, 2022.

[27] A. Carr, K. de Groot, M. Jansen, E. Bende, J. van Roosmalen, W. Eerenstein, R. Jonkman, R. van der Sanden, J. Bakker, B. de Gier and A. Harthoorn, "Tessera: Scalable, Shade Robust Module," in *IEEE 42nd Photovoltaic Specialist Conference*, New Orleans, LA, USA, 2015.

[28] S. Neven-du Mont, H. Alharthi, C. Kutter, H. Neuhaus and M. Heinrich, "Energy Yield Simulation of 3D Curved VIPV Modules," in *38th European Photovoltaic Solar Energy Conference and Exhibition*, Lisbon, Portugal, 221.

[29] "AN3432 Application Note," [Online]. Available: https://www.st.com/resource/en/application_note/an3432-how-to-choose-a-bypass-diode-for-silicon-panel-junction-box-stmicroelectronics.pdf. [Accessed 22 02 2024].

[30] A. J. Carr and B. K. Newman, "Expert Survey on Technical Requirements of PV-powered Passenger Vehicles," IEA PVPS, 2024.

[31] E. Klampaftis, D. Ross, G. Kocher-Oberlehner and B. S. Richards, "Integration of Color and Graphical Design for Photovoltaic Modules Using Luminescent Materials," *IEEE J. Photovolt.,* vol. 5, no. 2, pp. 584 - 590, 2015.

[32] "Technical details and certificates," Solaxess, [Online]. Available: https://www.solaxess.ch/en/photovoltaic-panels-pv/technical-details/. [Accessed 29 11 2023].

[33] "Vanceva® color PVB interlayers for laminated glass," Vanceva, [Online]. Available: https://www.vanceva.com/. [Accessed 29 11 2023].

[34] "Products for Decorative Glazing," Trosifol, [Online]. Available: https://www.trosifol.com/applications-products/decorative-glazing. [Accessed 29 11 2023].

[35] "High Efficiency Color PV Expert," LOF Solar Group, [Online]. Available: http://www.lofsolar.com/. [Accessed 21 02 2024].

[36] "RoyalGlam," KameleonSolar, [Online]. Available: https://kameleonsolar.com/products/royal-glam/. [Accessed 21 02 2024].

[37] "BISOL," BISOL, [Online]. Available: https://www.bisol.com/. [Accessed 21 02 2024].

[38] "Coloured Photovoltaic Panels," FuturaSun, [Online]. Available: https://www.futurasun.com/en/products/photovoltaic-monocrystalline-coloured-panels-silk-colour/. [Accessed 21 02 2024].

[39] "ColorQuant," Merck, [Online]. Available: https://www.merckgroup.com/en/expertise/effect-pigments/solutions/printing/pv-solar.html. [Accessed 21 02 2024].

[40] "Suncol BAPV," Sunage, [Online]. Available: https://sunage.ch/en/suncol-bapv. [Accessed 21 02 2024].

[41] "Kromatix PV Modules," Kromatix, [Online]. Available: https://kromatix.com/kromatix-pv-modules. [Accessed 21 02 2024].

[42] "Emirates Insolaire," Emirates Insolaire, [Online]. Available: https://emirates-insolaire.com/. [Accessed 21 02 2024].

[43] "Colored cells," KameleonSolar, [Online]. Available: https://kameleonsolar.com/products/#coloredcells. [Accessed 21 02 2024].

[44] "Color Blast," KameleonSolar, [Online]. Available: https://kameleonsolar.com/products/colorblast/. [Accessed 21 02 2024].

[45] "A new age of creative possibilities," ertex-solar, [Online]. Available: https://www.ertex-solar.at/en/company/know-how/. [Accessed 21 02 2024].

[46] "Solarix-Solar," Solarix-Solar, [Online]. Available: https://solarix-solar.com/en. [Accessed 21 02 2024].

[47] "ISSOL," ISSOL, [Online]. Available: http://www.issol.eu/. [Accessed 21 02 2024].

[48] "Steinfort," Steinfort Glas, [Online]. Available: https://steinfort.nl/. [Accessed 21 02 2024].

[49] "Colorful & Transparent Photovoltaic Panels," Solaronix, [Online]. Available: https://www.solaronix.com/. [Accessed 21 02 2024].

[50] "Heliatek," Heliatek, [Online]. Available: https://www.heliatek.com/. [Accessed 21 02 2024].

[51] "Catch the light," ASCA, [Online]. Available: https://www.asca.com/. [Accessed 21 02 2024].

[52] "Onyx Solar," Onyx Solar, [Online]. Available: https://onyxsolar.com/. [Accessed 21 02 2024].

[53] "SOLAXESS," SOLAXESS, [Online]. Available: https://www.solaxess.ch/en/home/. [Accessed 21 02 2024].

[54] "Souriez, vos photos créent de l'énergie," Bulletin Electrosuisse, [Online]. Available: https://www.bulletin.ch/fr/news-detail/souriez-vos-photos-creent-de-lenergie.html. [Accessed 22 02 2024].

[55] "Solar Visuals," Solar Visuals, [Online]. Available: https://www.solarvisuals.nl/. [Accessed 21 02 2024].

[56] "SunEwat Design," AGC, [Online]. Available: https://agc-activeglass.com/de/sunewat/sunewat-design/. [Accessed 21 02 2024].

[57] "Solar Curb Appeal," sistine solar, [Online]. Available: https://sistinesolar.com/. [Accessed 21 02 2024].

[58] "Skalafacade," Avancis GmbH, [Online]. Available: https://www.skalafacade.com/en/. [Accessed 21 02 2024].

[59] A. Borja Block, J. Escarre Palou, A. Faes, A. Virtuani and C. Ballif, "Accurate color characterization of solar photovoltaic modules for building integration," *Solar Energy,* vol. 267, p. 112227, 2024.

[60] "Tecglass," Tecglass, [Online]. Available: https://www.tecglassdigital.com/en/your-colors-on-glass-with-the-range-of-jetver-ceramic-inks. [Accessed 22 02 2024].

[61] J. Bing, L. Granados Caro, H. P. Talathi, N. L. Chang, D. R. Mckenzie and A. W. Y. Ho-Baillie, "Perovskite solar cells for building integrated photovoltaics—glazing applications," *Joule,* vol. 6, pp. 1446-1474, 2022.

[62] N. Patel, K. Bittkau, B. E. Pieters, E. Sovetkin, K. Ding and A. Reinders, "Impact of Additional PV Weight on the Energy Consumption of Electric Vehicles With Onboard PV," *IEEE J. Photovolt.,* pp. 319-329, 2024.

[63] A. Brooker, J. Gonder, L. Wang, E. Wood, S. Lopp and L. Ramroth, "FASTSim: A Model to Estimate Vehicle Efficiency, Cost and Performance," *SAE 2015 World Congress & Exhibition,* pp. 2015-01–0973, April 2015.

[64] A. Dobos, "PVWatts," NREL, [Online]. Available: https://pvwatts.nrel.gov/downloads/pvwattsv5.pdf.

[65] E. Wood, E. Burton, A. Duran and J. Gonder, "Appending High-Resolution Elevation Data to GPS Speed Traces for Vehicle Energy Modeling and Simulation," United States, https://doi.org/10.2172/1134504, 2014.

[66] W. F. Holmgren, C. W. Hansen and M. A. Mikofski, "pvlib python: a python package for modeling solar energy systems," *J. Open Source Software,* vol. 3, p. 884, 2018.

[67] M. O. Reese, S. Glynn, M. D. Kempe, D. L. McGott, M. S. Dabney, T. M. Barnes, S. Booth, D. Feldman and N. M. Haegel, "Increasing markets and decreasing package weight for high-specific-power photovoltaics," *Nature Energy,* vol. 3, pp. 1002-1012, 2018.

[68] "High Voltage DC/DC Converter - 4th Generation," Vitesco Technologies, [Online]. Available: https://www.vitesco-technologies.com/en-us/products/high-voltage-dc-dc-converter-4th-generation. [Accessed 22 02 2024].

[69] "22 kW 900 V Bidirectional DC-DC Converter," Fraunhofer IISB, [Online]. Available: https://www.iisb.fraunhofer.de/content/dam/iisb2014/en/Documents/Research-Areas/vehicle_electronics/Publications/DCDC_Converters/AutomotivePrototyping/brochure_22kw_900V_bidirectional_DCDC_Converter.pdf. [Accessed 22 02 2024].

[70] "Sunman," Sunman, [Online]. Available: https://www.sunman-energy.com/resources/. [Accessed 22 02 2024].

[71] "Solbian," [Online]. Available: https://solbian.solar/wp-content/uploads/2019/03/Datasheet-SP.pdf. [Accessed 22 02 2024].

[72] "Solbian," [Online]. Available: https://solbian.solar/wp-content/uploads/2019/11/Datasheet-SXX.pdf. [Accessed 22 02 2024].

[73] "FirstSolar," [Online]. Available: https://www.firstsolar.com/en-Emea/-/media/First-Solar/Technical-Documents/Series-6-Plus/Series-6-Plus-Datasheet---US.ashx?la=en-Emea. [Accessed 22 02 2024].

[74] "AltaDevices," AltaDevices, [Online]. Available: https://www.altadevices.com/. [Accessed 22 02 2024].

[75] "MiaSolé," [Online]. Available: https://miasole.com/wp-content/uploads/2022/07/solarridekit_datasheet.pdf. [Accessed 22 02 2024].

[76] A. Virtuani, D. Pavanello and G. Friesen, "Overview of temperature coefficients of different thin film photovoltaic technologies," in *25th European Photovoltaic Solar Energy Conference and Exhibition*, Valencia, 2010.

[77] E. Sovetkin, J. Noll, N. Patel, A. Gerber and B. E. Pieters, "Vehicle-Integrated Photovoltaics Irradiation Modeling Using Aerial-Based LIDAR Data and Validation with Trip Measurements," *Solar RRL,* vol. 7, p. 2200593, 2022.

[78] R. Peibst, H. Fischer, M. Brunner, A. Schießl, S. Wöhe, R. Wecker, F. Haase, H. Schulte-Huxel, S. Blankemeyer, M. Köntges, C. Hollemann, R. Brendel, G. Wetzel, J. Krügener, H. Nonnenmacher, H. Mehlich, A. Salavei, K. Ding, A. Lambertz, B. Pieters, S. Janke, B. Stannowski and L. Korte, "Demonstration of Feeding Vehicle-Integrated Photovoltaic-Converted Energy into the High-Voltage On-Board Network of Practical Light Commercial Vehicles for Range Extension," *Solar RRL,* vol. 6, p. 2100516, 2022.

[79] J. Markert, C. Kutter, B. Newman, P. Gebhardt and M. Heinrich, "Proposal for a Safety Qualification Program for Vehicle-Integrated PV Modules," *Sustainability,* vol. 13, p. 13341, 2021.

[80] Y. Ota, K. Araki, A. Nagaoka and K. Nishioka, "Facilitating vehicle-integrated photovoltaics by considering the radius of curvature of the roof surface for solar cell coverage," *Cleaner Engineering and Technology,* vol. 7, p. 100446, 2022.

[81] Y. Ota, K. Araki, A. Nagaoka and K. Nishioka, "Curve correction of vehicle-integrated photovoltaics using statistics on commercial car bodies," *Progress in Photovoltaics: Research and Applications,* vol. 30, pp. 152-163, 2022.

[82] "Vehicle-Integrated Photovoltaics," Fraunhofer ISE, [Online]. Available: https://www.ise.fraunhofer.de/en/key-topics/integrated-photovoltaics/vehicle-integrated-photovoltaics-vipv.html. [Accessed 22 12 2023].

[83] "Automotive OEMs," Sono Motors, [Online]. Available: https://sonomotors.com/. [Accessed 22 12 2023].

[84] "Vehicle Integrated PhotoVoltaics (VIPV)," CEA Liten, [Online]. Available: https://liten.cea.fr/cea-tech/liten/english/Pages/Medias/News/PV-Everywhere/Vehicle-Integrated-PhotoVoltaics.aspx. [Accessed 22 12 2023].

[85] "Vehicle integrated PV system for retractable car-roofs," pv magazine, [Online]. Available: https://www.pv-magazine.com/2023/09/21/vehicle-integrated-pv-system-for-retractable-car-roofs/. [Accessed 10 12 2023].

[86] "The freedom to go anywhere you want," aptera, [Online]. Available: https://aptera.us/vehicle/. [Accessed 22 12 2023].

[87] "Hyundai launches first car with solar roof charging system," Hyundai, [Online]. Available: https://www.hyundai.news/eu/articles/press-releases/hyundai-launches-first-car-with-solar-roof-charging-system.html. [Accessed 22 12 2023].

[88] K. Tékaya, "Curved infrared focal plane array : hemispherical forming and induced optoelectronic properties," 2014.

[89] "3S Solardach ☼ Kein Weg führt an der Sonnenenergie vorbei," 3S Swiss Solar Solutions AG, [Online]. Available: https://www.3s-solar.swiss/3s-solardach. [Accessed 29 11 2023].

[90] K. Araki, Y. Ota and K. Nishioka, "Modeling and rating the impact of partial shading loss affected by distributions of shading objects and orientation of PV modules (including moving PV in transportation), also design improvement of modules against partial and dynamic shading losses," in *33rd PVSEC Conference*, Nagoya, Japan, 2022.

[91] K. Araki, Y. Ota, A. Nagaoka and K. Nishioka, "Modeling and measurement of curved VIPV and BIPV modules – Impact of non-uniform solar irradiance and dynamic shading," in *34th PVSEC Conference*, Shenzhen, China, 2023.

[92] K. Araki, Y. Ota, A. Nagaoka and K. Nishioka, "3D-Curved crystalline Si modules: Size, Stress, Mismatching loss, and coverage loss," in *34th PVSEC Conference*, Shenzhen, China, 2023.